

## ELECTRONIC SUPPLEMENTARY INFORMATION

### Pressure-induced single-crystal-to-single crystal nitrite ligand isomerisation accompanied by a piezochromic effect

Kinga Potempa,<sup>a</sup> Damian Paliwoda,<sup>b</sup> Katarzyna N. Jarzemska,<sup>\*,a</sup>

Radosław Kamiński,<sup>a</sup> Adam Krówczyński,<sup>a</sup> Patryk Borowski,<sup>a</sup> Michael Hanfland<sup>c</sup>

<sup>a</sup> Department of Chemistry, University of Warsaw, Żwirki i Wigury 101, 02-089 Warsaw, Poland

<sup>b</sup> European Spallation Source ERIC, Partikelgatan 2, 224 84 Lund, Sweden

<sup>c</sup> European Synchrotron Radiation Facility, 71 avenue des Martyrs, 38043 Grenoble, France

\* Corresponding author: Katarzyna N. Jarzemska (katarzyna.jarzemska@uw.edu.pl)

### Table of contents

|   |     |
|---|-----|
| <b>1. Synthesis and compound characterization</b> ..... | S2  |
| 1.1. Synthesis .....                                    | S2  |
| 1.2. NMR and elemental analysis.....                    | S2  |
| <b>2. X-ray crystallography</b> .....                   | S4  |
| 2.1. Data collection.....                               | S4  |
| 2.2. Data processing .....                              | S4  |
| 2.3. Refinement .....                                   | S6  |
| <b>3. Crystal colour</b> .....                          | S11 |
| <b>4. Computational details</b> .....                   | S11 |
| <b>5. Structural and energetic analysis</b> .....       | S13 |
| <b>6. Pressure-induced structural changes</b> .....     | S24 |
| <b>7. Principal-axis strain-tensor analysis</b> .....   | S30 |
| <b>8. Theoretical UV-Vis spectra</b> .....              | S31 |
| <b>9. Additional references</b> .....                   | S32 |

## 1. Synthesis and compound characterization

**1.1. Synthesis.** All solvents and substrates were purchased from chemical companies and used without further purification. The synthesis is analogous to that described in literature (Campbell & Urbach, 1973) 7.3 mmol of pyridine-2-carbaldehyde was dissolved in 10 mL of isopropyl alcohol and added to a mixture of 3.8 mmol 1,3-diaminopropane in 10 mL of isopropyl alcohol cooled in an ice-water bath. Solution was stirred at room temperature for 1 hour and added to a hot solution of nickel(II) chloride hexahydrate (4.0 mmol). After solvent evaporation, green intermediate product was dissolved in 700 mL of methanol containing 50 mL of 2,2-dimethoxypropane. Solution of NaNO<sub>2</sub> (15 mmol) in 40 mL of methanol was added to the mixture. The final product was separated by filtration, washed with methanol and dried. Yield: 0.822 g (53%). Brownish-yellow crystals of **Ni-diONO** suitable for single-crystal X-ray diffraction experiments were obtained directly from synthesis.

**1.2. NMR and elemental analysis.** Nuclear magnetic resonance (NMR) spectra were measured with an Agilent NMR 400 MHz Varian spectrometer; <sup>1</sup>H chemical shifts are given relative to TMS by using residual solvent resonances. The <sup>1</sup>H NMR spectra show broadened signals which is a typical effect for paramagnetic samples – the Ni<sup>II</sup> metal centre in the studied **Ni-diONO** coordination compound adopts an octahedral coordination geometry and exhibits triplet electronic configuration in contrast to singlet square-planar nickel(II) complexes. The signal integrals agree well with the respective number of protons. Elemental analyses were carried out with an Elementar Vario EL III analyser. <sup>1</sup>H NMR (400 MHz, DMSO-d<sub>6</sub>) δ = 46.9 (br, 5H, Ar), 44.6 (br, 5H, Ar), 14.0 (br, 6H, –CH<sub>2</sub>–) ppm. Elemental analysis: C<sub>21</sub>H<sub>18</sub>N<sub>4</sub>NiO<sub>3</sub> (403.06); calculated: C 44.70%, H 4.00%, N 20.85%; found: C 44.56%, H 3.96%, N 20.59%.

| Parameter                | Value    |
|--------------------------|----------|
| 1 Solvent                | dms0     |
| 2 Temperature            | 25.0     |
| 3 Number of Scans        | 256      |
| 4 Spectrometer Frequency | 399.96   |
| 5 Spectral Width         | 119047.6 |
| 6 Nucleus                | 1H       |

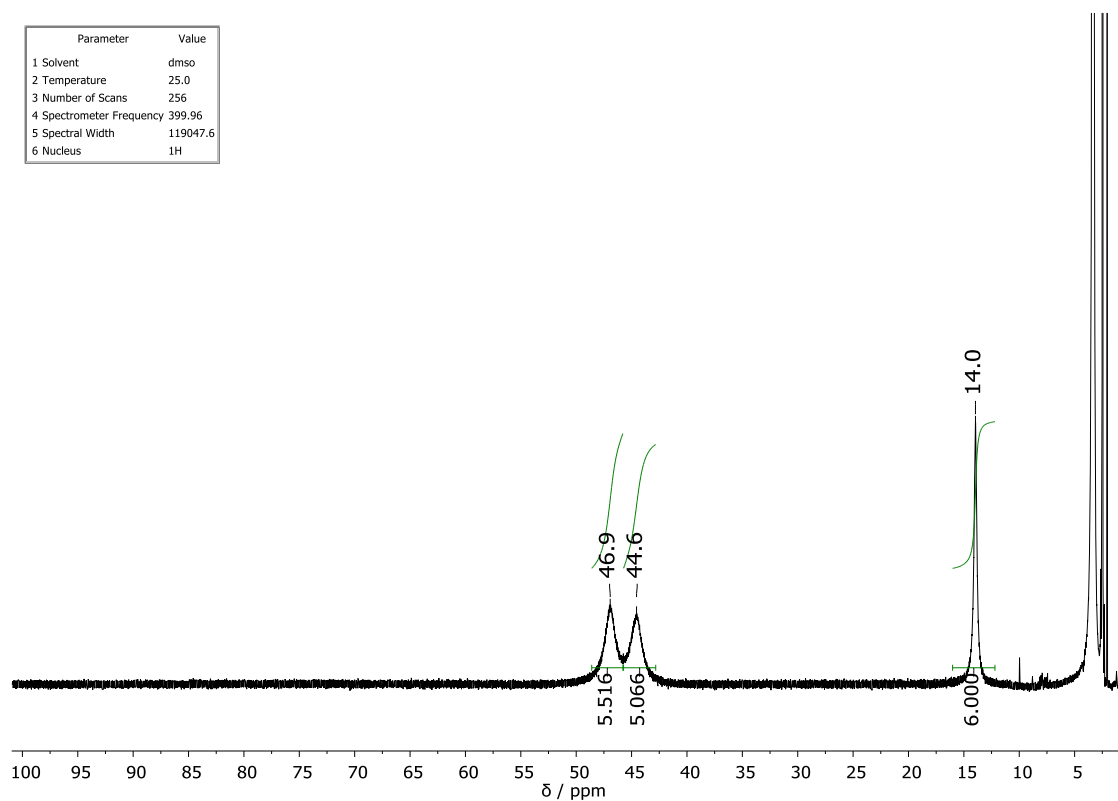


**Figure S1.1.** <sup>1</sup>H NMR spectrum of the **Ni-diONO** compound (400 MHz, DMSO-d<sub>6</sub>).

## 2. X-ray crystallography

**2.1. Data collection.** Standard multi-temperature X-ray diffraction experiments (including the preliminary ones) were carried out on a Rigaku Oxford Diffraction SuperNova single-crystal diffractometer equipped with a CCD detector, a molybdenum microfocus X-ray source, a low-temperature nitrogen gas flow Oxford Cryosystems device. In turn, a series of high-pressure X-ray diffraction experiments were performed at the ID15B beamline at the European Synchrotron Radiation Facility (ESRF), Grenoble, France. The sample was examined by a monochromatic X-ray beam with a working energy of 30 keV (0.41328 Å) focused to an area of approximately 30×30 μm<sup>2</sup>. Several single crystals of the **Ni-diONO** complex were loaded into the membrane-type diamond-anvil cell (DAC; 600 μm culet size Böhler-design diamonds from Almax easyLab) having an opening angle of 32°, together with a small ruby sphere. Stainless-steel gasket was used, which was previously pre-indented using exactly the same DAC, and next drilled with the electric discharge machine. Helium was utilized as a pressure transmission medium, whereas the pressure ruby luminescence (PRL) method was applied to monitor the pressure value inside the high-pressure chamber. Pressure was gradually increased from ambient to about 6.15(5) GPa with X-ray diffraction measurement performed at each subsequent pressure point (note the DAC was carefully checked for proper centring at each stage to ensure the best data quality possible). During the decompression a few X-ray diffraction measurements were additionally carried out, to see the sample response on the pressure release. More extensive data is presented in Table S2.1 below.

**2.2. Data processing.** Data processing (*i.e.*, unit-cell determination, raw diffraction-frame integration, absorption correction and scaling) was the same for all data sets collected, and were performed with the *CRYSTALISPRO* software (Rigaku Oxford Diffraction, 2024). For the synchrotron data specific masks were applied to take into account limited angular range of the DAC. Also, the reflections with unusual integration profiles were rejected, so as to eliminate the parasite X-ray scattering from the diamond anvils. During the integration, merging, scaling and absorption correction outliers were rejected, and at the final stage the determined space group information was taken into account. A particular attention was paid to the unit-cell choice, orientation-matrix transfer between data collections performed on the same crystals, and labelling of atoms within the asymmetric unit (ASU). As a result, not all cases are processed optimally in terms of the standard unit-cell choice, but our approach resulted in the data sets and

models easier to compare and discuss. In the case of several data sets of phase **II** and **III** some unit-cell angles are rather close to  $90^\circ$ . Therefore, various space-group-selection programs were occasionally suggesting higher metric symmetry. However, the intensity statistics clearly indicated the  $P\bar{1}$  space group as the correct one.

Data processing of the **Ni-diONO-06-I** data set proved to be a little more challenging. This data set is the last pressure point before the 1<sup>st</sup> HP-induced phase transition takes place;  $P = 2.15(5)$  GPa). When one is to determine the unit cell, only stronger reflections give the symmetry of the major component of the crystal, that is the phase **I**  $Cc$  space group. However, based on the reconstructed reciprocal layers it is well visible that some notably weaker reflections start to appear along the  $X^*$  direction (Figure S2.1). This is clearly a hint of the approaching phase transition to phase **II** exhibiting the  $P\bar{1}$  space group symmetry. Unfortunately, we were unable to take this effect into account during the data processing and subsequent model refinement. In turn, when the sample is compressed further to 2.88(2) GPa phase **I** is no longer observed, and phase **II** is the only crystal form present, with the elongated  $a$  unit-cell parameter and much more ‘skewed’ unit-cell shape (see the main text for further details).

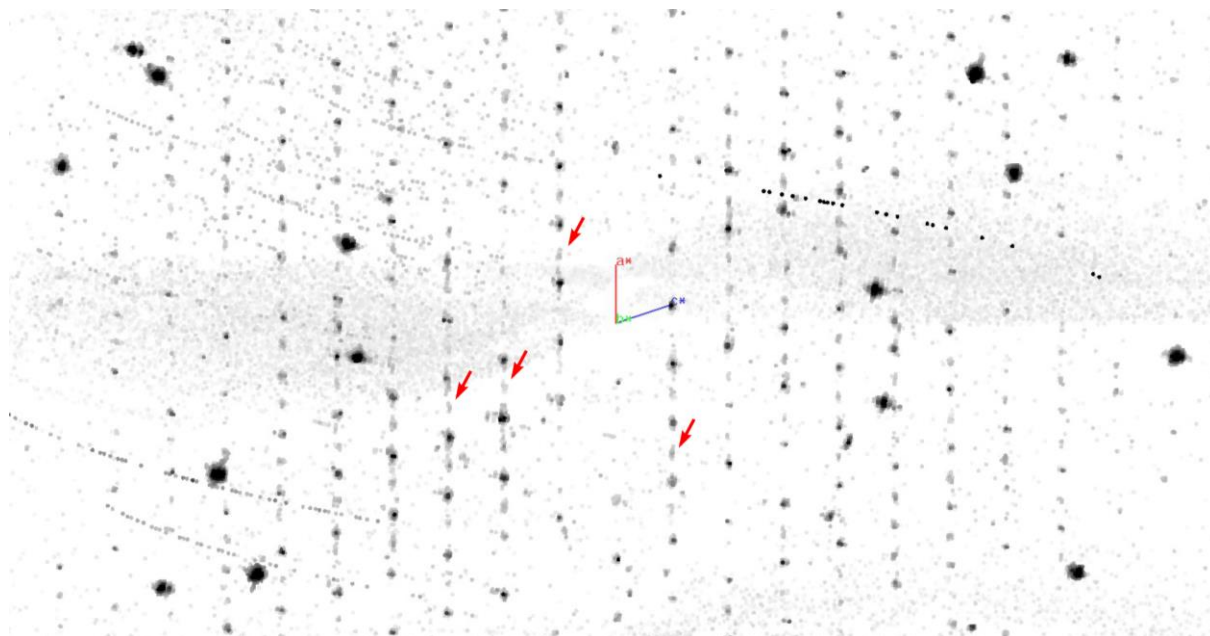


**Figure S2.1.** Reciprocal space visualization (*Ewald 3D* module of the *CRYSTALISPRO* program suite) showing weak Bragg reflections (selected peaks indicated with small arrows) appearing in-between phase **I** reflections along the  $X^*$  direction in the **Ni-diONO-06-I** data set. Large spots are the diamond-anvil reflections.

**2.3. Refinement.** All structures were solved using an intrinsic phasing method as implemented in the *SHELXT* program (Sheldrick, 2015) and refined with the *SHELXL* (Sheldrick, 2008) in the *OLEX2* package (Dolomanov *et al.*, 2009) within the independent atom model approximation. In some cases, *e.g.* in order to manipulate and transform the structure, the *JANA* program (Petříček *et al.*, 2014) was used. In all cases refinement was based on all unique reflections. As far as the disorder of the nitrite groups is concerned, all cases were treated separately, starting from an ordered model. Interestingly, some data points at r.t. show rather unstable refinement behaviour of these molecular fragments, which suggests the disorder may be somewhat dynamic in nature. For the sake of further computations and analysis we then applied reasonable sets of restraints and/or constraints, whenever justified and physically sound (our approach to find a stable model was guided by *e.g.* residual density map analyses). Finally, some reflections were omitted in the refinement, which is a standard practice in HP studies to overcome intrinsically lower data quality and possible diamond scattering.

The final comment refers to low-temperature data sets collected at the home source. Crystal structures of the **Ni-diONO** complex determined at 100 and 200 K exhibit *C2/c* space group, whereas the one collected at r.t. is properly solved and refined in the lower symmetry space group *Cc*. This is described in the main text and is the result of the minor disorder and switching of the NO<sub>2</sub> groups occurring at higher temperatures. Since the crystal packing in all these cases is nearly identical, in accordance with the *Cc* phase **I** studied further, the low-temperature *C2/c* phase is denoted as **I<sub>LT</sub>**.

The CIF files can be retrieved from the Cambridge Structural Database (deposition numbers: CCDC 2352765–83) (Allen, 2002, Groom *et al.*, 2016), or from ESI.

**Table S2.1.** Selected X-ray data collection, processing and refinement parameters for all reported crystal structures.

| <i>Data set</i>  | <b>Ni-diONO-100K-I-LT</b>   | <b>Ni-diONO-200K-I-LT</b> | <b>Ni-diONO-293K-I</b> | <b>Ni-diONO-01-I</b> | <b>Ni-diONO-02-I</b> | <b>Ni-diONO-03-I</b> | <b>Ni-diONO-04-I</b> |
|--|---|---------------------------|------------------------|----------------------|----------------------|----------------------|----------------------|
| Moiety formula   | C <sub>15</sub> H <sub>16</sub> N <sub>6</sub> Ni <sub>1</sub> O <sub>4</sub> |                           |                        |                      |                      |                      |                      |
| Formula mass, $M_r$ [ a.u. ]                               | 403.05  |                           |                        |                      |                      |                      |                      |
| Phase  | <b>I</b> <sub>LT</sub>  | <b>I</b> <sub>LT</sub>    | <b>I</b>               | <b>I</b>             | <b>I</b>             | <b>I</b>             | <b>I</b>             |
| Crystal system   | monoclinic  | monoclinic                | monoclinic             | monoclinic           | monoclinic           | monoclinic           | monoclinic           |
| Space group  | <i>C2/c</i> (No. 15)  | <i>C2/c</i> (No. 15)      | <i>Cc</i> (No. 9)      | <i>Cc</i> (No. 9)    | <i>Cc</i> (No. 9)    | <i>Cc</i> (No. 9)    | <i>Cc</i> (No. 9)    |
| $Z / Z'$   | 4 / ½   | 4 / ½                     | 4 / 1                  | 4 / 1                | 4 / 1                | 4 / 1                | 4 / 1                |
| $F_{000}$  | 832   | 832                       | 832                    | 832                  | 832                  | 832                  | 832                  |
| Crystal colour and/or shape                                | yellow plate  | yellow plate              | yellow plate           | colour not given †   | colour not given †   | colour not given †   | colour not given †   |
| Crystal size [ mm <sup>3</sup> ]                           | 0.15×0.19×0.26  | ← same crystal            | ← same crystal         | 0.13×0.07×0.02 ‡     | ← same crystal       | ← same crystal       | ← same crystal       |
| Temperature, $T$ [ K ]                                     | 100   | 200                       | rt.                    | rt.                  | rt.                  | rt.                  | rt.                  |
| Pressure, $P$ [ GPa ]                                      | ambient   | ambient                   | ambient                | ambient              | 0.40(5)              | 0.68(3)              | 1.08(3)              |
| $a$ [ Å ]  | 13.559(3)   | 13.643(3)                 | 13.750(3)              | 13.709(2)            | 13.5175(17)          | 13.385(3)            | 13.232(3)            |
| $b$ [ Å ]  | 9.666(2)  | 9.660(2)                  | 9.663(2)               | 9.662(3)             | 9.600(2)             | 9.559(2)             | 9.508(2)             |
| $c$ [ Å ]  | 13.263(3)   | 13.321(3)                 | 13.387(3)              | 13.361(3)            | 13.278(3)            | 13.218(3)            | 13.132(3)            |
| $\alpha$ [ ° ]   | 90  | 90                        | 90                     | 90                   | 90                   | 90                   | 90                   |
| $\beta$ [ ° ]  | 111.25(3)   | 111.02(3)                 | 110.53(3)              | 110.45(2)            | 110.466(16)          | 110.52(3)            | 110.46(3)            |
| $\gamma$ [ ° ]   | 90  | 90                        | 90                     | 90                   | 90                   | 90                   | 90                   |
| $V$ [ Å <sup>3</sup> ]                                     | 1620.1(7)   | 1638.7(7)                 | 1665.7(7)              | 1658.2(7)            | 1614.3(6)            | 1583.9(7)            | 1547.8(7)            |
| $d_{\text{calc}}$ [ g·cm <sup>-3</sup> ]                   | 1.652   | 1.634                     | 1.607                  | 1.614                | 1.658                | 1.690                | 1.730                |
| $\theta$ range   | 2.65–32.56°   | 2.65–32.46°               | 2.64–32.37°            | 1.83–21.16°          | 1.62–21.10°          | 1.63–21.25°          | 1.64–21.16°          |
| X-ray source   | Mo microfocus tube  | Mo microfocus tube        | Mo microfocus tube     | synchrotron          | synchrotron          | synchrotron          | synchrotron          |
| Absorption coefficient, $\mu$ [ mm <sup>-1</sup> ]         | 1.235   | 1.221                     | 1.201                  | 0.279                | 0.286                | 0.292                | 0.299                |
| No. of reflections collected / unique                      | 4635 / 2635   | 4805 / 2682               | 4850 / 3522            | 2005 / 1815          | 2059 / 2048          | 2036 / 2024          | 1987 / 1977          |
| $R_{\text{int}}$   | 2.32%   | 2.03%                     | 2.47%                  | 2.94%                | 1.74%                | 2.58%                | 1.74%                |
| No. of reflections with $I > 2\sigma(I)$                   | 2316  | 2357                      | 2686                   | 1406                 | 1763                 | 1736                 | 1699                 |
| No. of parameters / restraints                             | 123 / 0   | 123 / 0                   | 301 / 120              | 277 / 270            | 277 / 270            | 249 / 229            | 249 / 229            |
| $R[F]$ ( $I > 2\sigma(I)$ )                                | 3.66%   | 3.41%                     | 4.27%                  | 5.61%                | 6.09%                | 5.50%                | 5.37%                |
| $wR[F^2]$ (all data)                                       | 8.72%   | 7.24%                     | 9.47%                  | 16.77%               | 17.16%               | 15.98%               | 15.13%               |
| $\rho_{\text{res}}^{\text{min/max}}$ [ e·Å <sup>-3</sup> ] | -0.83 / +0.48   | -0.28 / +0.40             | -0.37 / +0.56          | -0.45 / +0.44        | -0.77 / +0.69        | -0.90 / +0.71        | -0.89 / +0.74        |
| CCDC code  | 2352765   | 2352766                   | 2352767                | 2352768              | 2352769              | 2352770              | 2352771              |

† Crystal colour not visible under experimental conditions due to the *in situ* PRL setup installed at the ESRF ID15B beamline. Separate colour measurements were done. ‡ Estimated.

**Table S2.1 (continued).** Selected X-ray data collection, processing and refinement parameters for all reported crystal structures.

| <i>Data set</i>   | <b>Ni-diONO-05-I</b> | <b>Ni-diONO-06-I</b> | <b>Ni-diONO-07-II</b>      | <b>Ni-diONO-08-II</b>      | <b>Ni-diONO-09-III</b>     | <b>Ni-diONO-10- III</b>    | <b>Ni-diONO-11- III</b>    |
|---|----------------------|----------------------|----------------------------|----------------------------|----------------------------|----------------------------|----------------------------|
| Phase   | <b>I</b>             | <b>I</b>             | <b>II</b>                  | <b>II</b>                  | <b>III</b>                 | <b>III</b>                 | <b>III</b>                 |
| Crystal system  | monoclinic           | monoclinic           | triclinic                  | triclinic                  | triclinic                  | triclinic                  | triclinic                  |
| Space group   | <i>Cc</i> (No. 9)    | <i>Cc</i> (No. 9)    | <i>P</i> $\bar{1}$ (No. 2) | <i>P</i> $\bar{1}$ (No. 2) | <i>P</i> $\bar{1}$ (No. 2) | <i>P</i> $\bar{1}$ (No. 2) | <i>P</i> $\bar{1}$ (No. 2) |
| <i>Z</i> / <i>Z'</i>  | 4 / 1                | 4 / 1                | 6 / 3                      | 6 / 3                      | 4 / 2                      | 4 / 2                      | 4 / 2                      |
| <i>F</i> <sub>000</sub>                                       | 832                  | 832                  | 1248                       | 1248                       | 832                        | 832                        | 832                        |
| Crystal colour and/or shape                                   | colour not given †   | colour not given †   | colour not given †         | colour not given †         | colour not given †         | colour not given †         | colour not given †         |
| Crystal size [ mm <sup>3</sup> ]                              | ← same crystal       | ← same crystal       | ← same crystal             | ← same crystal             | ← same crystal             | ← same crystal             | ← same crystal             |
| Temperature, <i>T</i> [ K ]                                   | rt.                  | rt.                  | rt.                        | rt.                        | rt.                        | rt.                        | rt.                        |
| Pressure, <i>P</i> [ GPa ]                                    | 1.73(3)              | 2.15(5)              | 2.88(2)                    | 3.33(3)                    | 3.98(2)                    | 4.58(2)                    | 5.38(3)                    |
| <i>a</i> [ Å ]  | 13.026(3)            | 12.836(3)            | 19.686(4)                  | 19.543(4)                  | 12.396(2)                  | 12.306(3)                  | 12.208(3)                  |
| <i>b</i> [ Å ]  | 9.450(2)             | 9.391(2)             | 9.307(2)                   | 9.269(2)                   | 9.204(2)                   | 9.1663(8)                  | 9.1260(11)                 |
| <i>c</i> [ Å ]  | 13.021(3)            | 12.908(3)            | 12.765(3)                  | 12.708(3)                  | 12.618(3)                  | 12.558(3)                  | 12.491(3)                  |
| $\alpha$ [ ° ]  | 90                   | 90                   | 90.02(3)                   | 89.99(3)                   | 90.26(3)                   | 90.212(12)                 | 90.205(14)                 |
| $\beta$ [ ° ]   | 110.40(3)            | 108.56(3)            | 106.67(3)                  | 106.56(3)                  | 105.54(3)                  | 105.34(2)                  | 105.14(2)                  |
| $\gamma$ [ ° ]  | 90                   | 90                   | 105.24(3)                  | 105.39(3)                  | 87.17(3)                   | 87.125(13)                 | 87.019(15)                 |
| <i>V</i> [ Å <sup>3</sup> ]                                   | 1502.3(6)            | 1475.1(6)            | 2154.4(9)                  | 2120.2(9)                  | 1385.3(5)                  | 1364.3(5)                  | 1341.4(5)                  |
| <i>d</i> <sub>calc</sub> [ g·cm <sup>-3</sup> ]               | 1.782                | 1.815                | 1.864                      | 1.894                      | 1.933                      | 1.962                      | 1.996                      |
| $\theta$ range  | 1.66–21.42°          | 1.68–21.18°          | 1.56–21.40°                | 1.57–21.54°                | 1.57–21.53°                | 1.58–21.63°                | 1.59–21.74°                |
| X-ray source  | synchrotron          | synchrotron          | synchrotron                | synchrotron                | synchrotron                | synchrotron                | synchrotron                |
| Absorption coefficient,<br>$\mu$ [ mm <sup>-1</sup> ]         | 0.308                | 0.313                | 0.322                      | 0.327                      | 0.334                      | 0.339                      | 0.345                      |
| No. of reflections<br>collected / unique                      | 1888 / 1882          | 1889 / 1882          | 5543 / 5543                | 5464 / 3730                | 3546 / 2408                | 3546 / 2406                | 3526 / 2390                |
| <i>R</i> <sub>int</sub>                                       | 6.83%                | 2.54%                | 4.17%                      | 3.72%                      | 7.51%                      | 7.52%                      | 7.53%                      |
| No. of reflections with<br><i>I</i> > 2 $\sigma$ ( <i>I</i> ) | 1593                 | 1295                 | 2649                       | 2667                       | 1409                       | 1410                       | 1391                       |
| No. of parameters<br>/ restraints                             | 249 / 229            | 277 / 246            | 669 / 585                  | 669 / 610                  | 421 / 342                  | 421 / 336                  | 421 / 288                  |
| <i>R</i> [ <i>F</i> ] ( <i>I</i> > 2 $\sigma$ ( <i>I</i> ))   | 6.31%                | 7.93%                | 6.07%                      | 6.13%                      | 9.25%                      | 9.36%                      | 9.34%                      |
| <i>wR</i> [ <i>F</i> <sup>2</sup> ] (all data)                | 18.48%               | 25.69%               | 18.10%                     | 17.67%                     | 26.83%                     | 27.21%                     | 27.14%                     |
| $\rho_{\text{res}}^{\text{min/max}}$ [ e·Å <sup>-3</sup> ]    | -0.83 / +0.86        | -0.59 / +0.65        | -0.52 / +0.62              | -0.52 / +0.62              | -0.61 / +0.86              | -0.63 / +0.86              | -0.58 / +0.82              |
| CCDC code   | 2352772              | 2352773              | 2352774                    | 2352775                    | 2352776                    | 2352777                    | 2352778                    |



**Table S2.1 (continued).** Selected X-ray data collection, processing and refinement parameters for all reported crystal structures.

| <i>Data set</i>  | <b>Ni-diONO-12-III</b> | <b>Ni-diONO-13-III</b> | <b>Ni-diONO-14-II</b> | <b>Ni-diONO-15-II</b> | <b>Ni-diONO-16-I</b> |
|--|------------------------|------------------------|-----------------------|-----------------------|----------------------|
| Phase  | <b>III</b>             | <b>III</b>             | <b>II</b>             | <b>II</b>             | <b>I</b>             |
| Crystal system   | triclinic              | triclinic              | triclinic             | triclinic             | monoclinic           |
| Space group  | $P\bar{1}$ (No. 2)     | $P\bar{1}$ (No. 2)     | $P\bar{1}$ (No. 2)    | $P\bar{1}$ (No. 2)    | $Cc$ (No. 9)         |
| $Z / Z'$   | 4 / 2                  | 4 / 2                  | 6 / 3                 | 6 / 3                 | 4 / 1                |
| $F_{000}$  | 832                    | 832                    | 1248                  | 1248                  | 832                  |
| Crystal colour and/or shape                                | colour not given †     | colour not given †     | colour not given †    | colour not given †    | colour not given †   |
| Crystal size [ mm <sup>3</sup> ]                           | ← same crystal         | ← same crystal         | ← same crystal        | ← same crystal        | ← same crystal       |
| Temperature, $T$ [ K ]                                     | rt.                    | rt.                    | rt.                   | rt.                   | rt.                  |
| Pressure, $P$ [ GPa ]                                      | 6.15(5)                | 4.1(1)                 | 3.30(5)               | 2.28(2)               | 0.93(3)              |
| $a$ [ Å ]  | 12.098(2)              | 12.369(3)              | 19.527(2)             | 19.770(2)             | 13.295(3)            |
| $b$ [ Å ]  | 9.0718(10)             | 9.1988(13)             | 9.2591(9)             | 9.3295(8)             | 9.5267(13)           |
| $c$ [ Å ]  | 12.404(2)              | 12.599(2)              | 12.693(2)             | 12.7960(17)           | 13.169(3)            |
| $\alpha$ [ ° ]   | 90.129(12)             | 90.252(13)             | 90.057(10)            | 90.044(9)             | 90                   |
| $\beta$ [ ° ]  | 104.909(16)            | 105.495(17)            | 106.512(11)           | 106.801(10)           | 110.60(2)            |
| $\gamma$ [ ° ]   | 87.038(12)             | 87.182(14)             | 105.351(12)           | 104.937(10)           | 90                   |
| $V$ [ Å <sup>3</sup> ]                                     | 1313.7(3)              | 1379.7(5)              | 2114.6(5)             | 2175.8(4)             | 1561.3(6)            |
| $d_{\text{calc}}$ [ g·cm <sup>-3</sup> ]                   | 2.038                  | 1.940                  | 1.899                 | 1.846                 | 1.715                |
| $\theta$ range   | 1.60–21.88°            | 1.60–21.55°            | 1.57–21.58°           | 1.56–21.33°           | 1.99–21.24°          |
| X-ray source   | synchrotron            | synchrotron            | synchrotron           | synchrotron           | synchrotron          |
| Absorption coefficient,<br>$\mu$ [ mm <sup>-1</sup> ]      | 0.352                  | 0.335                  | 0.328                 | 0.319                 | 0.296                |
| No. of reflections<br>collected / unique                   | 3541 / 2402            | 3440 / 2340            | 5430 / 3701           | 5630 / 3827           | 1943 / 1838          |
| $R_{\text{int}}$   | 7.54%                  | 12.59%                 | 3.03%                 | 3.55%                 | 3.21%                |
| No. of reflections with<br>$I > 2\sigma(I)$                | 1400                   | 1205                   | 2775                  | 2751                  | 1584                 |
| No. of parameters<br>/ restraints                          | 421 / 366              | 421 / 438              | 669 / 646             | 669 / 646             | 277 / 246            |
| $R[F]$ ( $I > 2\sigma(I)$ )                                | 9.63%                  | 7.38%                  | 6.30%                 | 6.70%                 | 6.19%                |
| $wR[F^2]$ (all data)                                       | 28.09%                 | 24.04%                 | 18.87%                | 20.40%                | 17.52%               |
| $\rho_{\text{res}}^{\text{min/max}}$ [ e·Å <sup>-3</sup> ] | -0.59 / +0.87          | -0.37 / +0.37          | -0.63 / +0.72         | -0.58 / +0.77         | -0.72 / +0.72        |
| CCDC code  | 2352779                | 2352780                | 2352781               | 2352782               | 2352783              |

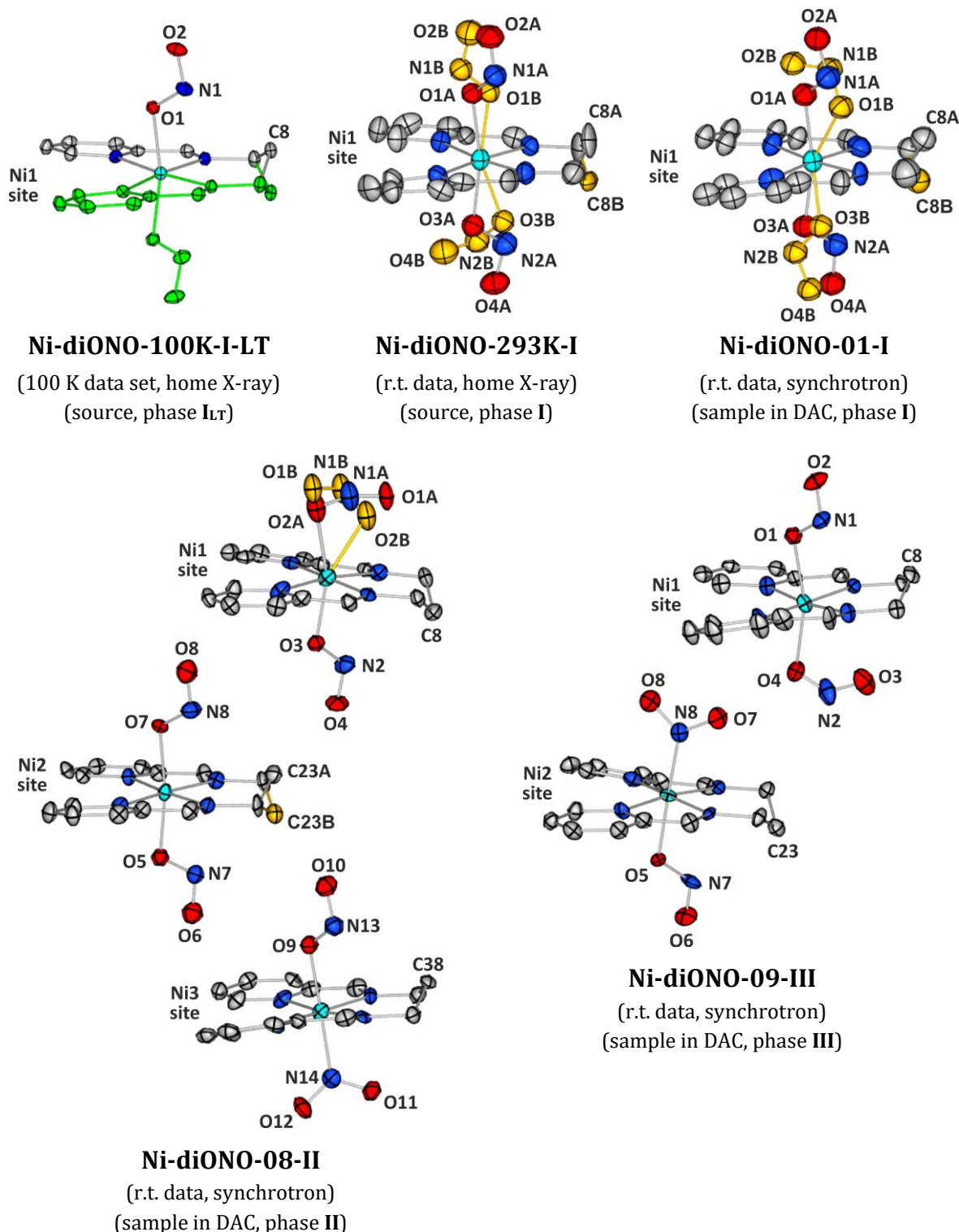


**Figure S2.2.** Molecular structures and ASU contents in the crystal structures of the studied **Ni-diONO** compound derived from the X-ray diffraction data as shown in Table S2.1. Atomic thermal motion is represented as ellipsoids at the 50% probability level, while hydrogen atoms are omitted for clarity. Only essential atomic labels are retained for clarity. Ni1 site is always chosen with the same orientation. Disordered parts are shown in gold (gold colour always represents the minor part – part “B”). For the 100 K structure in phase I<sub>Lr</sub> the symmetry-equivalent part of the molecule is shown in green.

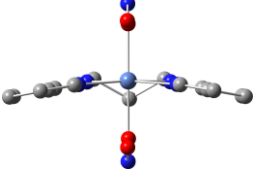
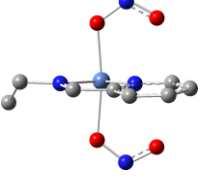
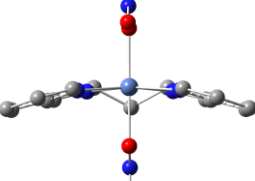
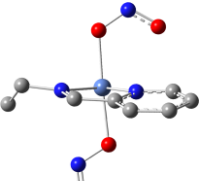
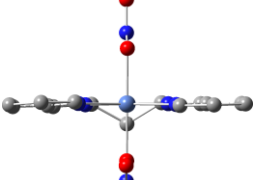
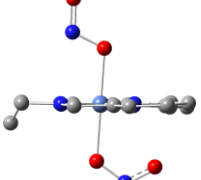
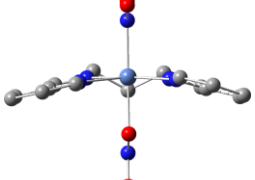
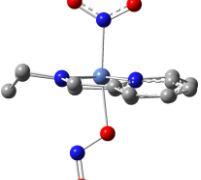
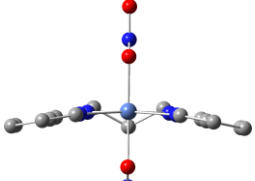
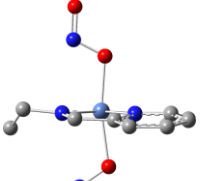
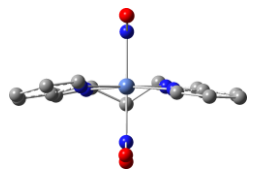
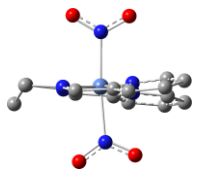
### 3. Crystal colour

Due to the presence of the PRL device installed at the ID15B beamline recording of crystal's colour was not possible. Therefore, the crystal's colour at various pressure points was monitored separately using the small home-made Merrill-Basset DAC (MB-DAC) available in our laboratory. The single crystal was placed in the MB-DAC together with a small ruby sphere. Stainless-steel 200  $\mu\text{m}$  thickness gasket was used. The pressure was measured with the RubyLux PRL device (Almax easyLab) and the colour changes were recorded with the laboratory stereoscopic microscope with digital camera (Olympus).

### 4. Computational details

Isolated-molecule, dimer interaction energies, and normal-mode frequencies were calculated using the density functional theory (DFT) at the DFT(B3LYP)/6-311++G\*\* level of theory (McLean & Chandler, 1980, Clark *et al.*, 1983, Perdew, 1986, Becke, 1988, Lee *et al.*, 1988) using the *GAUSSIAN* package (ver. 16) (Frisch *et al.*, 2016). In the case of interaction energy calculations, the Grimme empirical dispersion correction (Grimme, 2004, 2006) modified by the Becke-Johnson damping function (Grimme *et al.*, 2010, Grimme *et al.*, 2011) and correction for basis set superposition error (Boys & Bernardi, 1970) were applied. The UV-Vis spectra of all linkage isomers were also computed at the same level of theory, *i.e.* DFT(B3LYP)/6-311++G\*\*. The semi-automatic generation of input files was accomplished with our local *CLUSTERGEN* program (Kamiński *et al.*, 2013).

**Table S4.1.** Relative energy ( $E_{\text{rel}}$ ) values between possible **Ni-diONO** linkage isomers computed for the optimised isolated-molecule geometries. It is worth noting that the ancillary ligand conformation is changed depending on the nitrite isomers present in the structures.

| Nitrite isomer *                            | $E_{\text{rel}}$ [ kJ·mol <sup>-1</sup> ] | Front view  | Side view   |
|---|---|---|---|
| <i>endo</i> -nitrito / <i>endo</i> -nitrito | 0.00                                      |    |    |
| <i>endo</i> -nitrito / <i>exo</i> -nitrito  | +11.43                                    |    |    |
| <i>exo</i> -nitrito / <i>endo</i> -nitrito  | +12.31                                    |   |   |
| <i>nitro</i> / <i>exo</i> -nitrito          | +13.71                                    |  |  |
| <i>exo</i> -nitrito / <i>exo</i> -nitrito   | +28.72                                    |  |  |
| <i>nitro</i> / <i>nitro</i>                 | +2.95                                     |  |  |

\* The isomers are described as follows: isomer No. 1 / isomer No. 2, where isomer No. 1 is the nitrite moiety on the opposite side of the plane defined by the ancillary ligand with respect to the C8 molecular tip, and isomer No 2 is the nitrite moiety on the same side of the plane defined by the ancillary ligand with respect to the C8 molecular tip.

## 5. Structural and energetic analysis

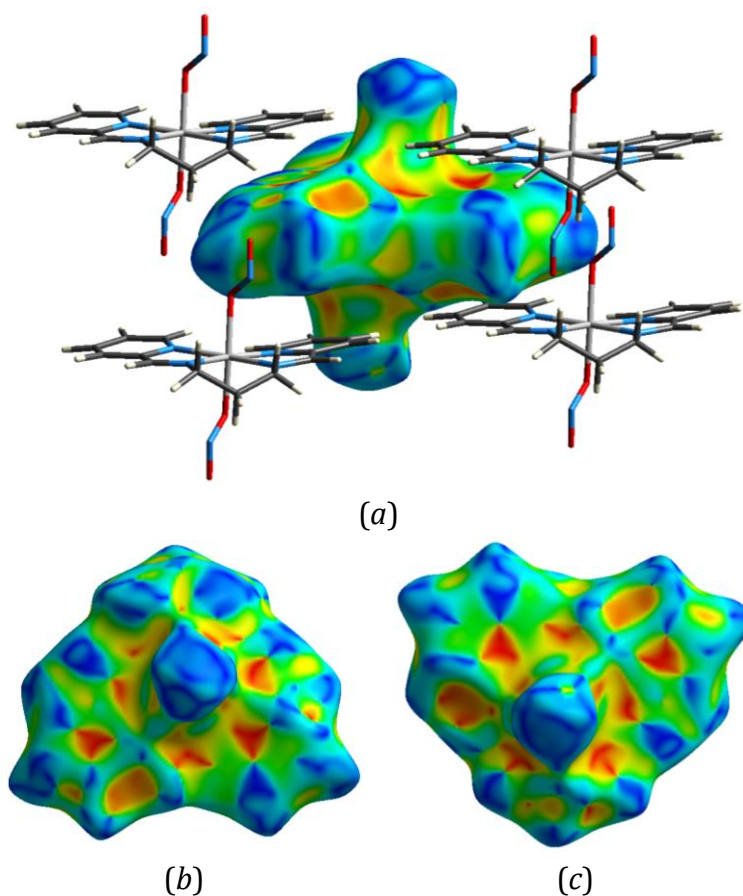


**Figure S5.1.** Hirshfeld surface generated for the **Ni-diONO** complex at 100 K mapped with the shape index property (Spackman & Jayatilaka, 2009). It indicates the presence of the interactions between aromatic fragments of a given molecule and its four neighbours in the crystal structure (a).  $\pi$ -stacking is visualized by characteristic triangular hollows (orange) and bumps (blue) on the surface: (b) view from above and (c) view from the below.

**Comment.** Reaction cavities (Figure S5.2) increase with the temperature, and also they occupy more of the unit-cell volume (though changes are not large). At 100 K their volume is equal to  $V_{\text{cav}} = 227.08 \text{ \AA}^3$  (14% of the unit-cell volume;  $28.39 \text{ \AA}^3$  per single molecule in ASU), whereas at 200 K –  $V_{\text{cav}} = 242.42 \text{ \AA}^3$  (14.8% of the unit-cell volume;  $30.30 \text{ \AA}^3$  per single molecule in ASU), and finally at r.t. –  $V_{\text{cav}} = 273.22 \text{ \AA}^3$  (16.4% of the unit-cell volume). At 100 and 200 K only one type of reaction cavities is observed, due to the symmetry of the crystal. At r.t. the two sides of the molecule differentiate and the respective reaction cavities become different. Reaction cavity for the –O1–N1=O2 group amounts to  $140.73 \text{ \AA}^3$  ( $35.18 \text{ \AA}^3$  per single molecule in ASU), and for the –O3–N2=O4 to  $132.49 \text{ \AA}^3$  ( $33.12 \text{ \AA}^3$  per single molecule in ASU).

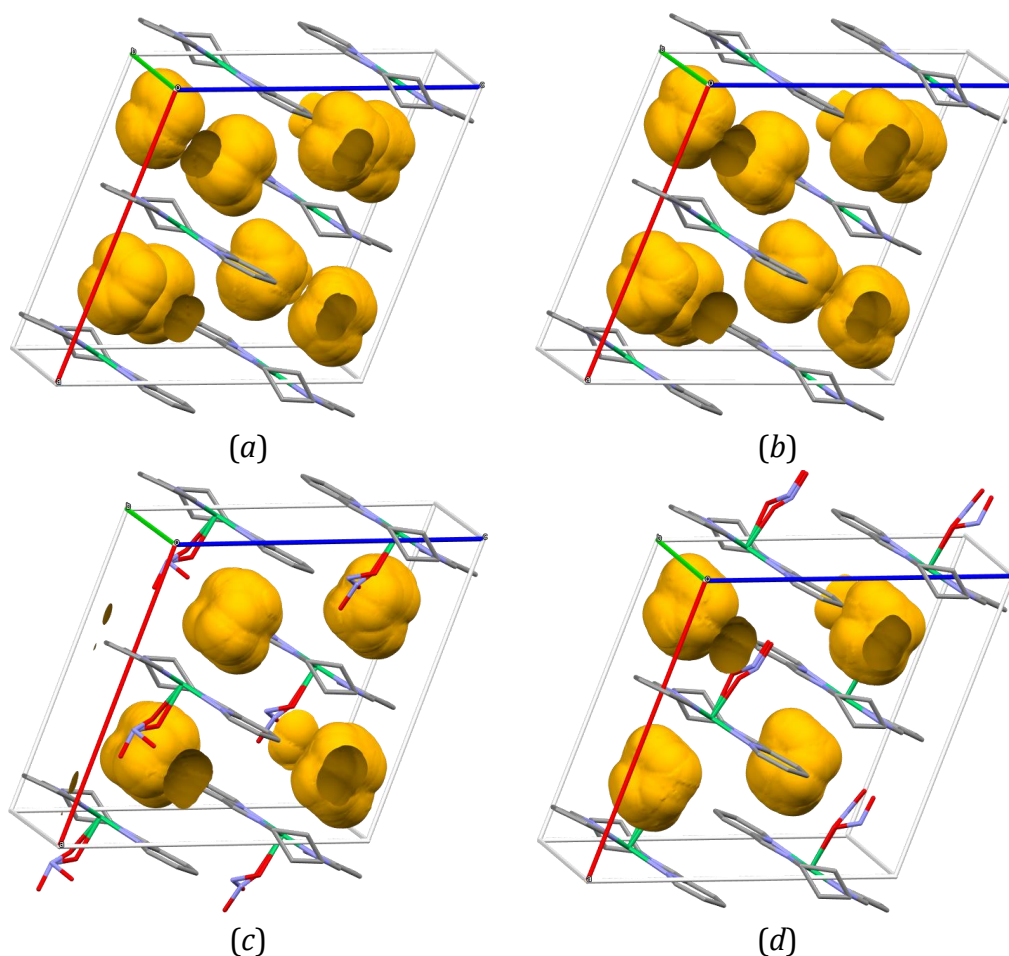


**Figure S5.2.** Reaction cavities calculated and generated with the *MERCURY* program (probe radius: 1.2 Å, grid spacing: 0.1 Å, selected NO<sub>2</sub> groups cut-out) for multi-temperature measurements: (a) 100 K, (b) 200 K, (c) r.t. for the -O1-N1=O<sub>2</sub> group, (c) r.t. for the -O3-N2=O<sub>4</sub> group.

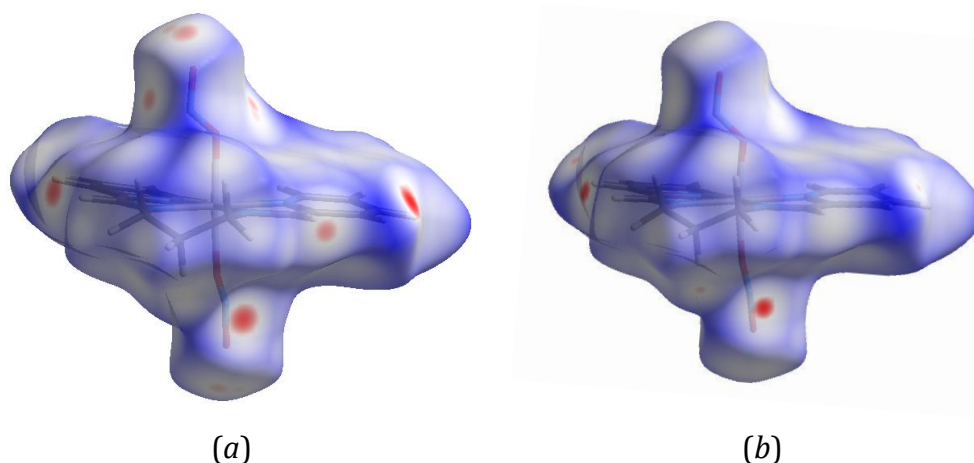


**Figure S5.3.** Hirshfeld surface generated for **Ni-diONO** at 100 K (a) and at r.t. (b) mapped with the  $d_{\text{norm}}$  property (Spackman & Jayatilaka, 2009). Upon heating the surface volume increased from 397.56 to 409.71 Å<sup>3</sup>. Intermolecular interactions between adjacent molecules are getting weaker, which is visualized by fading red dots on the Hirshfeld surface.

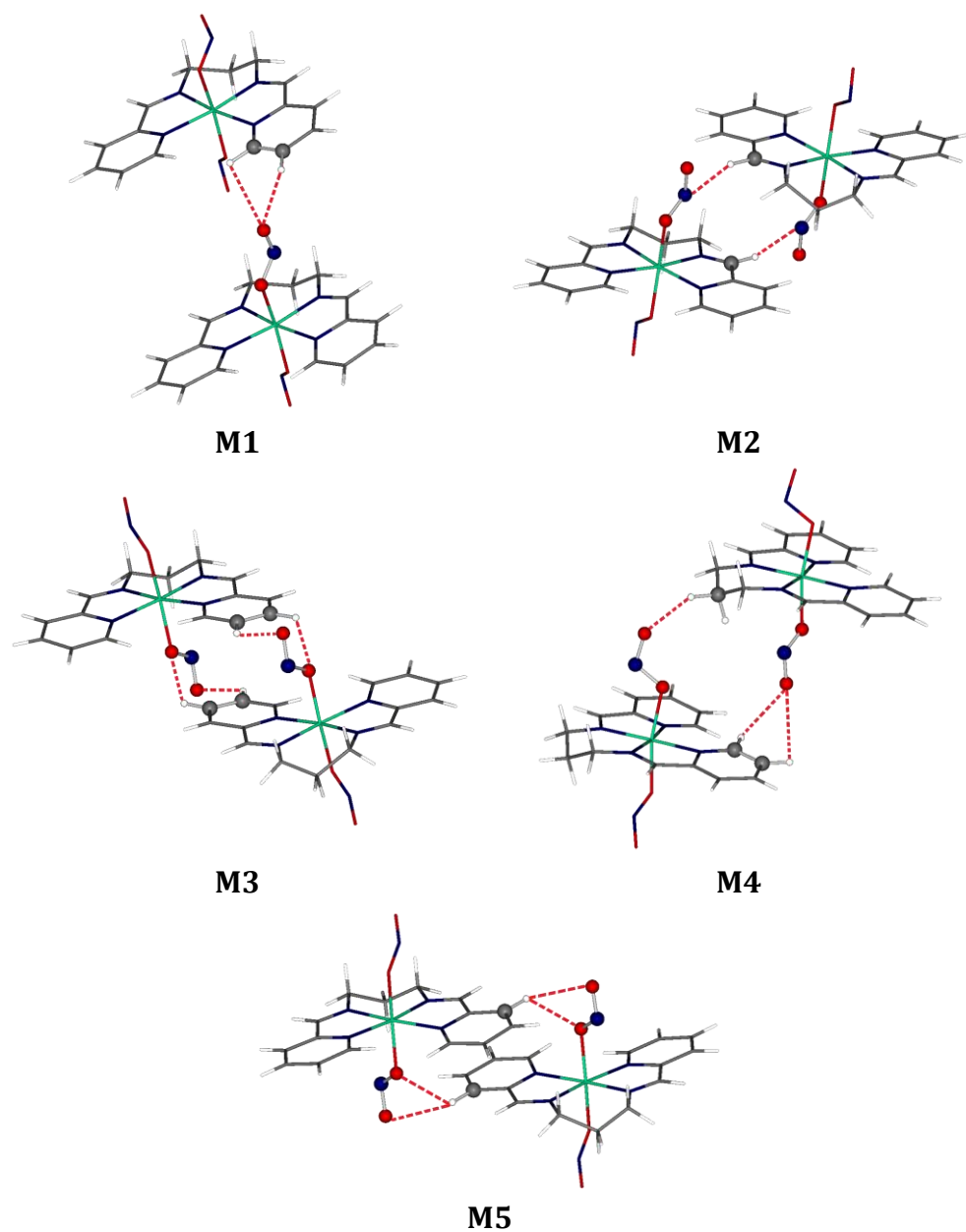


**Figure S5.4.** Main dimeric motifs encountered for each isomeric form in the **Ni-diONO** crystal structure at 100 K and under ambient pressure. For interaction energies see Table S5.1.

**Table S5.1.** Major dimeric motifs and respective interaction energies ( $E_{\text{int}}$ 's) calculated at the DFT(B3LYP)/6-311++G\*\* level of theory based on the crystal structure at 100 K. Corrections for dispersion and BSSE were applied. For visualization of the motifs see Figure S5.4.

| <i>Motif</i> | $E_{\text{int}}$ [kJ·mol <sup>-1</sup> ] | <i>Selected interactions</i> | $d_{\text{D-H}}$ [Å] | $d_{\text{H...A}}$ [Å] | $d_{\text{D...A}}$ [Å] | $\theta_{\text{D-H...A}}$ [°] |
|--------------|--|------------------------------|----------------------|------------------------|------------------------|-------------------------------|
| <b>M1</b>    | -43.30                                   | O2...H1-C1 <sup>#1</sup>     | 1.077                | 2.804                  | 3.123                  | 97.13                         |
|              |  | O2...H2-C2 <sup>#1</sup>     | 1.077                | 2.890                  | 3.161                  | 94.41                         |
| <b>M2</b>    | -70.00                                   | N1...H10-C10 <sup>#2</sup>   | 1.077                | 2.477                  | 3.517                  | 162.21                        |
|              |  | N2...H6-C6 <sup>#2</sup>     | 1.077                | 2.472                  | 3.525                  | 165.47                        |
|              |  | C8...H4-C4 <sup>#2</sup>     | 1.077                | 2.901                  | 3.613                  | 123.79                        |
| <b>M3</b>    | -78.80                                   | O1...H13-C13 <sup>#3</sup>   | 1.077                | 2.640                  | 3.374                  | 124.91                        |
|              |  | O2...H14-C14 <sup>#3</sup>   | 1.077                | 2.607                  | 3.447                  | 134.35                        |
|              |  | O3...H3-C3 <sup>#3</sup>     | 1.077                | 2.623                  | 3.372                  | 126.11                        |
|              |  | O4...H2-C2 <sup>#3</sup>     | 1.077                | 2.536                  | 3.377                  | 134.26                        |
| <b>M4</b>    | -43.85                                   | O2...8b-C8 <sup>#4</sup>     | 1.083                | 2.811                  | 3.375                  | 112.49                        |
|              |  | O4...H14-C14 <sup>#4</sup>   | 1.077                | 2.953                  | 3.192                  | 92.76                         |
|              |  | O4...H15-C15 <sup>#4</sup>   | 1.077                | 2.788                  | 3.123                  | 97.83                         |
| <b>M5</b>    | -92.42                                   | O1...H4-C4 <sup>#5</sup>     | 1.077                | 2.429                  | 3.169                  | 124.74                        |
|              |  | O2...H4-C4 <sup>#5</sup>     | 1.077                | 2.571                  | 3.370                  | 130.33                        |
|              |  | O3...H12-C12 <sup>#5</sup>   | 1.077                | 2.422                  | 3.167                  | 125.17                        |
|              |  | O4...H12-C12 <sup>#5</sup>   | 1.077                | 2.609                  | 3.393                  | 129.08                        |

Symmetry operations: (#1)  $x-\frac{1}{2}, y+\frac{1}{2}, z$ ; (#2)  $x+1, -y+1, z+\frac{1}{2}$ ; (#3)  $x, -y, z+\frac{1}{2}$ ; (#4)  $x+\frac{1}{2}, y+\frac{1}{2}, z$ ; (#5)  $x-\frac{1}{2}, -y+\frac{1}{2}, z-\frac{1}{2}$ .



**Table S5.2.** Major dimeric motifs and respective interaction energies ( $E_{\text{int}}$ 's) calculated at the DFT(B3LYP)/6-311++G\*\* level of theory based on the crystal structure at 200 K. Corrections for dispersion and BSSE were applied.

| <i>Motif</i> | $E_{\text{int}}$ [kJ·mol <sup>-1</sup> ] | <i>Selected interactions</i> | $d_{\text{D-H}}$ [Å] | $d_{\text{H...A}}$ [Å] | $d_{\text{D...A}}$ [Å] | $\theta_{\text{D-H...A}}$ [°] |
|--------------|--|------------------------------|----------------------|------------------------|------------------------|-------------------------------|
| <b>M1</b>    | -42.22                                   | O2...H1-C1 <sup>#1</sup>     | 1.077                | 2.826                  | 3.167                  | 98.33                         |
|              |  | O2...H2-C2 <sup>#1</sup>     | 1.077                | 2.931                  | 3.180                  | 93.27                         |
| <b>M2</b>    | -70.29                                   | N1...H10-C10 <sup>#2</sup>   | 1.077                | 2.461                  | 3.518                  | 166.77                        |
|              |  | N2...H6-C6 <sup>#2</sup>     | 1.077                | 2.529                  | 3.567                  | 161.31                        |
|              |  | C8...H4-C4 <sup>#2</sup>     | 1.077                | 3.933                  | 3.640                  | 123.49                        |
| <b>M3</b>    | -76.86                                   | O1...H13-C13 <sup>#3</sup>   | 1.077                | 2.646                  | 3.481                  | 126.61                        |
|              |  | O2...H14-C14 <sup>#3</sup>   | 1.077                | 2.612                  | 3.463                  | 135.44                        |
|              |  | O3...H3-C3 <sup>#3</sup>     | 1.077                | 2.750                  | 3.475                  | 124.40                        |
|              |  | O4...H2-C2 <sup>#3</sup>     | 1.077                | 2.582                  | 3.407                  | 132.87                        |
| <b>M4</b>    | -44.10                                   | O2...8b-C8 <sup>#4</sup>     | 1.083                | 2.813                  | 3.405                  | 114.33                        |
|              |  | O4...H14-C14 <sup>#4</sup>   | 1.077                | 2.952                  | 3.227                  | 94.85                         |
|              |  | O4...H15-C15 <sup>#4</sup>   | 1.077                | 2.871                  | 3.174                  | 96.25                         |
| <b>M5</b>    | -91.21                                   | O1...H4-C4 <sup>#5</sup>     | 1.077                | 2.459                  | 3.203                  | 125.21                        |
|              |  | O2...H4-C4 <sup>#5</sup>     | 1.077                | 2.654                  | 3.444                  | 129.84                        |
|              |  | O3...H12-C12 <sup>#5</sup>   | 1.077                | 2.454                  | 3.196                  | 124.99                        |
|              |  | O4...H12-C12 <sup>#5</sup>   | 1.077                | 2.634                  | 3.422                  | 129.51                        |

Symmetry operations: (#1)  $x-1/2, y+1/2, z$ ; (#2)  $x+1, -y+1, z+1/2$ ; (#3)  $x, -y, z+1/2$ ; (#4)  $x+1/2, y+1/2, z$ ; (#5)  $x-1/2, -y+1/2, z-1/2$ .

**Table S5.3.** Major dimeric motifs and respective interaction energies ( $E_{\text{int}}$ 's) calculated at the DFT(B3LYP)/6-311++G\*\* level of theory based on the crystal structure at r.t. for the double *exo*-nitrito isomer. Corrections for dispersion and BSSE were applied.

| <i>Motif</i> | $E_{\text{int}}$ [kJ·mol <sup>-1</sup> ] | <i>Selected interactions</i> | $d_{\text{D-H}}$ [Å] | $d_{\text{H...A}}$ [Å] | $d_{\text{D...A}}$ [Å] | $\theta_{\text{D-H...A}}$ [°] |
|--------------|--|------------------------------|----------------------|------------------------|------------------------|-------------------------------|
| <b>M1</b>    | -45.81                                   | O2...H1-C1 <sup>#1</sup>     | 1.077                | 2.955                  | 3.292                  | 98.56                         |
|              |  | O2...H2-C2 <sup>#1</sup>     | 1.077                | 2.983                  | 3.300                  | 97.42                         |
| <b>M2</b>    | -71.42                                   | N1...H10-C10 <sup>#2</sup>   | 1.077                | 2.519                  | 3.573                  | 165.80                        |
|              |  | N2...H6-C6 <sup>#2</sup>     | 1.077                | 2.503                  | 3.543                  | 162.19                        |
|              |  | C8...H4-C4 <sup>#2</sup>     | 1.077                | 2.965                  | 3.627                  | 120.09                        |
| <b>M3</b>    | -73.97                                   | O1...H13-C13 <sup>#3</sup>   | 1.077                | 2.866                  | 3.583                  | 124.22                        |
|              |  | O2...H14-C14 <sup>#3</sup>   | 1.077                | 2.630                  | 3.443                  | 131.83                        |
|              |  | O3...H3-C3 <sup>#3</sup>     | 1.077                | 2.780                  | 3.530                  | 126.64                        |
|              |  | O4...H2-C2 <sup>#3</sup>     | 1.077                | 2.658                  | 3.512                  | 135.82                        |
| <b>M4</b>    | -42.17                                   | O2...8b-C8 <sup>#4</sup>     | 1.083                | 3.015                  | 3.416                  | 102.45                        |
|              |  | O4...H14-C14 <sup>#4</sup>   | 1.077                | 2.922                  | 3.191                  | 94.37                         |
|              |  | O4...H15-C15 <sup>#4</sup>   | 1.077                | 2.953                  | 3.227                  | 94.84                         |
| <b>M5</b>    | -89.33                                   | O1...H4-C4 <sup>#5</sup>     | 1.077                | 2.649                  | 3.281                  | 125.87                        |
|              |  | O2...H4-C4 <sup>#5</sup>     | 1.077                | 2.850                  | 3.519                  | 129.88                        |
|              |  | O3...H12-C12 <sup>#5</sup>   | 1.077                | 2.546                  | 3.223                  | 129.92                        |
|              |  | O4...H12-C12 <sup>#5</sup>   | 1.077                | 2.783                  | 3.504                  | 135.11                        |

Symmetry operations: (#1)  $x-1/2, y+1/2, z$ ; (#2)  $x+1, -y+1, z+1/2$ ; (#3)  $x, -y, z+1/2$ ;  
 (#4)  $x+1/2, y+1/2, z$ ; (#5)  $x-1/2, -y+1/2, z-1/2$ .

**Table S5.4.** Major dimeric motifs and respective interaction energies ( $E_{\text{int}}$ 's) calculated at the DFT(B3LYP)/6-311++G\*\* level of theory based on the crystal structure at r.t. for the double *endo*-nitrito isomer. Corrections for dispersion and BSSE were applied.

| <i>Motif</i> | $E_{\text{int}}$ [kJ·mol <sup>-1</sup> ] | <i>Selected interactions</i> | $d_{\text{D-H}}$ [Å] | $d_{\text{H...A}}$ [Å] | $d_{\text{D...A}}$ [Å] | $\theta_{\text{D-H...A}}$ [°] |
|--------------|--|------------------------------|----------------------|------------------------|------------------------|-------------------------------|
| <b>M1</b>    | -18.70                                   | N1...H1-C1 <sup>#1</sup>     | 1.077                | 4.160                  | 4.543                  | 104.03                        |
|              |  | N1...H2-C2 <sup>#1</sup>     | 1.077                | 4.141                  | 4.524                  | 104.00                        |
|              |  | O4...H9b-C9                  | 1.083                | 2.863                  | 3.946                  | 177.17                        |
| <b>M2</b>    | -50.63                                   | O1...H10-C10 <sup>#2</sup>   | 1.077                | 3.221                  | 4.237                  | 157.67                        |
|              |  | N2...H6-C6 <sup>#2</sup>     | 1.077                | 2.788                  | 3.768                  | 151.30                        |
|              |  | C8...H4-C4 <sup>#2</sup>     | 1.077                | 2.965                  | 3.627                  | 120.09                        |
| <b>M3</b>    | -32.76                                   | N1...H14-C14 <sup>#3</sup>   | 1.077                | 2.507                  | 3.152                  | 117.48                        |
|              |  | O2...H13-C13 <sup>#3</sup>   | 1.077                | 1.767                  | 2.683                  | 140.08                        |
|              |  | N2...H2-C2 <sup>#3</sup>     | 1.077                | 2.311                  | 3.111                  | 129.63                        |
|              |  | O4...H3-C3 <sup>#3</sup>     | 1.077                | 1.873                  | 2.676                  | 128.08                        |
| <b>M4</b>    | -18.70                                   | O2...8a-C8 <sup>#4</sup>     | 1.083                | 3.396                  | 3.886                  | 109.02                        |
|              |  | N2...H14-C14 <sup>#4</sup>   | 1.077                | 4.049                  | 4.348                  | 98.93                         |
|              |  | N2...H15-C15 <sup>#4</sup>   | 1.077                | 4.321                  | 4.505                  | 92.88                         |
| <b>M5</b>    | -83.97                                   | O1...H4-C4 <sup>#5</sup>     | 1.077                | 2.689                  | 3.209                  | 109.22                        |
|              |  | O2...H4-C4 <sup>#5</sup>     | 1.077                | 2.087                  | 3.092                  | 154.10                        |
|              |  | O3...H12-C12 <sup>#5</sup>   | 1.077                | 3.305                  | 3.871                  | 114.06                        |
|              |  | O4...H12-C12 <sup>#5</sup>   | 1.077                | 2.300                  | 3.294                  | 152.55                        |

Symmetry operations: (#1)  $x-1/2, y+1/2, z$ ; (#2)  $x+1, -y+1, z+1/2$ ; (#3)  $x, -y, z+1/2$ ;  
 (#4)  $x+1/2, y+1/2, z$ ; (#5)  $x-1/2, -y+1/2, z-1/2$ .

**Table S5.5.** Overview of interaction energies ( $E_{\text{int}}$ 's) calculated at the DFT(B3LYP)/6-311++G\*\* level of theory for each generated dimeric motif possible at r.t. Sum of interaction energies for all motifs present in the given case is denoted as  $\Sigma$ . Note that the first isomer given in the table header is located at the opposite side of the plane of the tetradentate ligand with respect to the C8 tip.

| <i>Motif</i> | <i>exo-nitrito</i>   | <i>endo-nitrito</i>   | <i>exo-nitrito</i>    | <i>endo-nitrito</i>  |
|--------------|----------------------|-----------------------|-----------------------|----------------------|
|              | / <i>exo-nitrito</i> | / <i>endo-nitrito</i> | / <i>endo-nitrito</i> | / <i>exo-nitrito</i> |
| <b>M1</b>    | -45.81               | -18.70                | -34.48                | -29.46               |
| <b>M2</b>    | -71.42               | -50.63                | -60.80                | -58.49               |
| <b>M3</b>    | -73.97               | -32.76                | -55.02                | -51.51               |
| <b>M4</b>    | -42.17               | -18.70                | -28.78                | -27.82               |
| <b>M5</b>    | -89.33               | -83.97                | -83.43                | -89.37               |
| $\Sigma$     | -322.70              | -204.76               | -262.51               | -256.65              |

**Table S5.6.** Major dimeric motifs and respective interaction energies ( $E_{\text{int}}$ 's) calculated at the DFT(B3LYP)/6-311++G\*\* level of theory based on the crystal structure at 2.15(5) GPa for the double *exo-nitrito* isomer. Corrections for dispersion and BSSE were applied.

| <i>Motif</i> | $E_{\text{int}}$ [kJ·mol <sup>-1</sup> ] | <i>Selected interactions</i> | $d_{\text{D-H}}$ [Å] | $d_{\text{H...A}}$ [Å] | $d_{\text{D...A}}$ [Å] | $\theta_{\text{D-H...A}}$ [°] |
|--------------|--|------------------------------|----------------------|------------------------|------------------------|-------------------------------|
| <b>M1</b>    | -48.70                                   | O2...H1-C1 <sup>#1</sup>     | 1.077                | 2.671                  | 2.951                  | 94.16                         |
|              |  | O2...H2-C2 <sup>#1</sup>     | 1.077                | 2.748                  | 2.991                  | 92.30                         |
| <b>M2</b>    | -65.94                                   | N1...H10-C10 <sup>#2</sup>   | 1.077                | 2.519                  | 3.562                  | 162.65                        |
|              |  | N2...H6-C6 <sup>#2</sup>     | 1.077                | 2.298                  | 3.358                  | 167.77                        |
|              |  | C8...H4-C4 <sup>#2</sup>     | 1.077                | 2.624                  | 3.346                  | 123.84                        |
| <b>M3</b>    | -75.19                                   | O1...H13-C13 <sup>#3</sup>   | 1.077                | 2.431                  | 3.159                  | 123.80                        |
|              |  | O2...H14-C14 <sup>#3</sup>   | 1.077                | 2.494                  | 3.292                  | 130.12                        |
|              |  | O3...H3-C3 <sup>#3</sup>     | 1.077                | 2.654                  | 3.370                  | 123.43                        |
|              |  | O4...H2-C2 <sup>#3</sup>     | 1.077                | 2.573                  | 3.448                  | 137.75                        |
| <b>M4</b>    | -43.72                                   | O2...8b-C8 <sup>#4</sup>     | 1.083                | 2.512                  | 3.040                  | 108.95                        |
|              |  | O4...H14-C14 <sup>#4</sup>   | 1.077                | 2.712                  | 2.814                  | 84.09                         |
|              |  | O4...H15-C15 <sup>#4</sup>   | 1.077                | 2.560                  | 2.732                  | 87.38                         |
| <b>M5</b>    | -84.73                                   | O1...H4-C4 <sup>#5</sup>     | 1.077                | 2.373                  | 3.143                  | 127.18                        |
|              |  | O2...H4-C4 <sup>#5</sup>     | 1.077                | 2.506                  | 3.308                  | 130.45                        |
|              |  | O3...H12-C12 <sup>#5</sup>   | 1.077                | 2.382                  | 3.140                  | 126.15                        |
|              |  | O4...H12-C12 <sup>#5</sup>   | 1.077                | 2.718                  | 3.491                  | 128.50                        |

Symmetry operations: (#1)  $x-1/2, y+1/2, z$ ; (#2)  $x+1, -y+1, z+1/2$ ; (#3)  $x, -y, z+1/2$ ; (#4)  $x+1/2, y+1/2, z$ ; (#5)  $x-1/2, -y+1/2, z-1/2$ .

**Table S5.7.** Major dimeric motifs and respective interaction energies ( $E_{\text{int}}$ 's) calculated at the DFT(B3LYP)/6-311++G\*\* level of theory based on the crystal structure at 2.15(5) GPa for the *endo*-nitrito / *exo*-nitrito isomer. Corrections for dispersion and BSSE were applied.

| <i>Motif</i> | $E_{\text{int}}$ [kJ·mol <sup>-1</sup> ] | <i>Selected interactions</i> | $d_{\text{D-H}}$ [Å] | $d_{\text{H...A}}$ [Å] | $d_{\text{D...A}}$ [Å] | $\theta_{\text{D-H...A}}$ [°] |
|--------------|--|------------------------------|----------------------|------------------------|------------------------|-------------------------------|
| <b>M1</b>    | -14.43                                   | N1...H1-C1 <sup>#1</sup>     | 1.077                | 3.873                  | 4.051                  | 91.72                         |
|              |  | N1...H2-C2 <sup>#1</sup>     | 1.077                | 3.880                  | 4.056                  | 91.58                         |
| <b>M2</b>    | -53.81                                   | O2...H10-C10 <sup>#2</sup>   | 1.077                | 1.924                  | 2.971                  | 162.76                        |
|              |  | N2...H6-C6 <sup>#2</sup>     | 1.077                | 2.298                  | 3.358                  | 167.77                        |
|              |  | C8...H4-C4 <sup>#2</sup>     | 1.077                | 2.624                  | 3.346                  | 123.84                        |
| <b>M3</b>    | -59.91                                   | N1...H14-C14 <sup>#3</sup>   | 1.077                | 2.452                  | 3.277                  | 132.55                        |
|              |  | O1...H13-C13 <sup>#3</sup>   | 1.077                | 2.524                  | 3.262                  | 124.91                        |
|              |  | O3...H3-C3 <sup>#3</sup>     | 1.077                | 2.654                  | 3.370                  | 123.43                        |
|              |  | O4...H2-C2 <sup>#3</sup>     | 1.077                | 2.573                  | 3.448                  | 137.75                        |
| <b>M4</b>    | -17.15                                   | O2...8a-C8 <sup>#4</sup>     | 1.083                | 3.273                  | 3.980                  | 123.90                        |
|              |  | O4...H14-C14 <sup>#4</sup>   | 1.077                | 2.712                  | 2.814                  | 84.09                         |
|              |  | O4...H15-C15 <sup>#4</sup>   | 1.077                | 2.560                  | 2.732                  | 87.38                         |
| <b>M5</b>    | -78.45                                   | O1...H4-C4 <sup>#5</sup>     | 1.077                | 2.318                  | 3.067                  | 125.13                        |
|              |  | O2...H3-C3 <sup>#5</sup>     | 1.077                | 2.133                  | 3.011                  | 136.96                        |
|              |  | O3...H12-C12 <sup>#5</sup>   | 1.077                | 2.382                  | 3.140                  | 126.15                        |
|              |  | O4...H12-C12 <sup>#5</sup>   | 1.077                | 2.718                  | 3.491                  | 128.50                        |

Symmetry operations: (#1)  $x-\frac{1}{2}, y+\frac{1}{2}, z$ ; (#2)  $x+1, -y+1, z+\frac{1}{2}$ ; (#3)  $x, -y, z+\frac{1}{2}$ ; (#4)  $x+\frac{1}{2}, y+\frac{1}{2}, z$ ; (#5)  $x-\frac{1}{2}, -y+\frac{1}{2}, z-\frac{1}{2}$ .

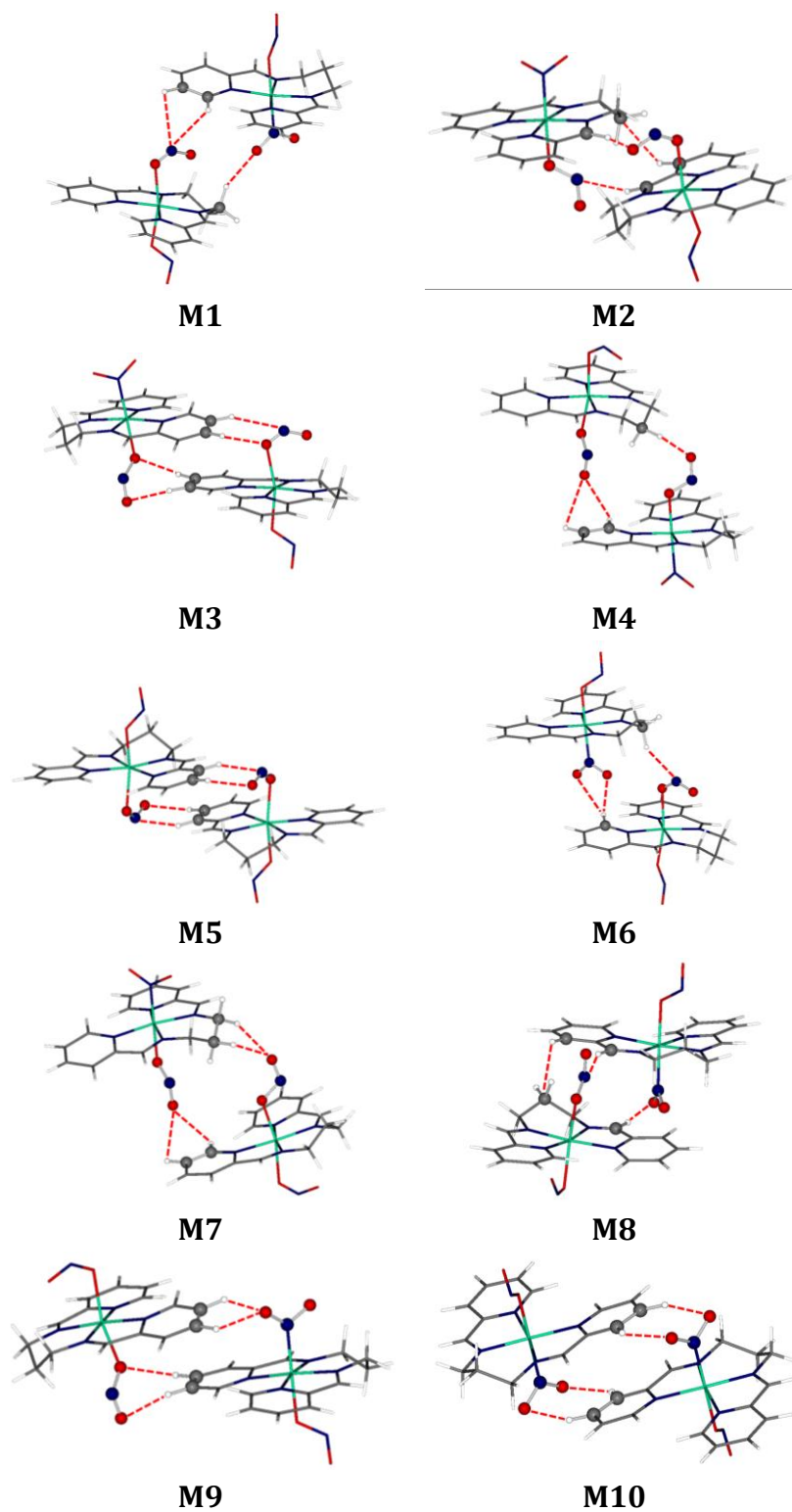


**Figure S5.5.** Main dimeric motifs encountered for each isomeric form in the **Ni-diONO** crystal structure at 3.98(2) GPa and at room temperature. For interaction energies see Table S5.8.

**Table S5.8.** Major dimeric motifs and respective interaction energies ( $E_{\text{int}}$ 's) calculated at the DFT(B3LYP)/6-311++G\*\* level of theory based on the crystal structure at 3.98(2) GPa. Corrections for dispersion and BSSE were applied. For visualization of the motifs see Figure S5.5.

| <i>Motif</i> | $E_{\text{int}}$ [kJ·mol <sup>-1</sup> ] | <i>Selected interactions</i> | $d_{\text{D-H}}$ [Å] | $d_{\text{H...A}}$ [Å] | $d_{\text{D...A}}$ [Å] | $\theta_{\text{D-H...A}}$ [°] |
|--------------|--|------------------------------|----------------------|------------------------|------------------------|-------------------------------|
| <b>M1</b>    | -33.85                                   | N8...H14-C14 <sup>#1</sup>   | 1.077                | 2.768                  | 3.217                  | 104.84                        |
|              |  | N8...H15-C15 <sup>#1</sup>   | 1.077                | 3.768                  | 3.271                  | 97.77                         |
|              |  | O4...H24B-C24                | 1.083                | 2.337                  | 3.363                  | 157.52                        |
| <b>M2</b>    | -52.46                                   | O8...H10-C10 <sup>#2</sup>   | 1.077                | 2.146                  | 3.142                  | 152.83                        |
|              |  | N1...H21-C21 <sup>#2</sup>   | 1.077                | 2.306                  | 3.514                  | 147.23                        |
|              |  | C8...H19-C19 <sup>#2</sup>   | 1.077                | 2.619                  | 3.225                  | 114.97                        |
| <b>M3</b>    | -57.99                                   | N8...H14-C14 <sup>#3</sup>   | 1.077                | 2.922                  | 3.722                  | 131.24                        |
|              |  | O7...H13-C13 <sup>#3</sup>   | 1.077                | 2.325                  | 3.010                  | 119.82                        |
|              |  | O1...H18-C18 <sup>#3</sup>   | 1.077                | 2.336                  | 3.087                  | 125.36                        |
|              |  | O2...H17-C17 <sup>#3</sup>   | 1.077                | 2.507                  | 3.306                  | 130.26                        |
| <b>M4</b>    | -33.39                                   | O2...23A-C23 <sup>#4</sup>   | 1.083                | 2.365                  | 2.993                  | 115.37                        |
|              |  | O6...H2-C2 <sup>#4</sup>     | 1.077                | 2.818                  | 2.920                  | 84.56                         |
|              |  | O6...H1-C1 <sup>#4</sup>     | 1.077                | 2.786                  | 2.924                  | 86.49                         |
| <b>M5</b>    | -55.19                                   | N8...H27-C27 <sup>#5</sup>   | 1.077                | 2.531                  | 3.320                  | 129.30                        |
|              |  | O8...H28-C28 <sup>#5</sup>   | 1.077                | 2.255                  | 3.060                  | 130.00                        |
| <b>M6</b>    | -40.21                                   | N8...H9B-C9                  | 1.083                | 2.488                  | 3.464                  | 149.26                        |
|              |  | O3...H30-C30                 | 1.077                | 2.653                  | 3.155                  | 79.94                         |
|              |  | O4...H30-C30                 | 1.077                | 2.858                  | 2.873                  | 107.90                        |
| <b>M7</b>    | -31.59                                   | O2...H16-C16 <sup>#6</sup>   | 1.077                | 2.767                  | 2.877                  | 84.78                         |
|              |  | O2...H17-C17 <sup>#6</sup>   | 1.077                | 2.662                  | 2.835                  | 87.95                         |
|              |  | O6...H7A-C7 <sup>#6</sup>    | 1.083                | 2.491                  | 3.203                  | 122.26                        |
|              |  | O6...H8A-C8 <sup>#6</sup>    | 1.083                | 2.432                  | 3.016                  | 112.41                        |
| <b>M8</b>    | -62.68                                   | O3...H25-C25 <sup>#7</sup>   | 1.077                | 2.306                  | 3.514                  | 147.23                        |
|              |  | N7...H6-C6 <sup>#7</sup>     | 1.077                | 2.146                  | 3.142                  | 152.83                        |
|              |  | C23...H4-C4 <sup>#7</sup>    | 1.077                | 2.619                  | 3.225                  | 114.97                        |
| <b>M9</b>    | -67.95                                   | O4...H28-C28 <sup>#8</sup>   | 1.077                | 2.125                  | 3.914                  | 127.89                        |
|              |  | O4...H29-C29 <sup>#8</sup>   | 1.077                | 2.625                  | 3.148                  | 109.20                        |
|              |  | O5...H3-C3 <sup>#8</sup>     | 1.077                | 2.345                  | 3.097                  | 125.54                        |
|              |  | O6...H2-C2 <sup>#8</sup>     | 1.077                | 2.588                  | 3.342                  | 126.44                        |
| <b>M10</b>   | -73.16                                   | O3...H13-C13 <sup>#9</sup>   | 1.077                | 2.258                  | 3.050                  | 128.75                        |
|              |  | O4...H12-C12 <sup>#9</sup>   | 1.077                | 2.303                  | 3.296                  | 152.51                        |

Symmetry operations: (#1)  $x, y-1, z$ ; (#2)  $-x+1, -y+1, -z+1$ ; (#3)  $-x+1, -y+2, -z+1$ ;  
 (#4)  $x+1, y-1, z$ ; (#5)  $-x+1, -y+1, -z$ ; (#6)  $x+1, y, z$ ; (#7)  $-x+1, -y+1, -z$ ; (#8)  $-x+1, -y+2, -z$ ;  
 (#9)  $-x+1, -y+2, -z-1$ .

## 6. Pressure-induced structural changes

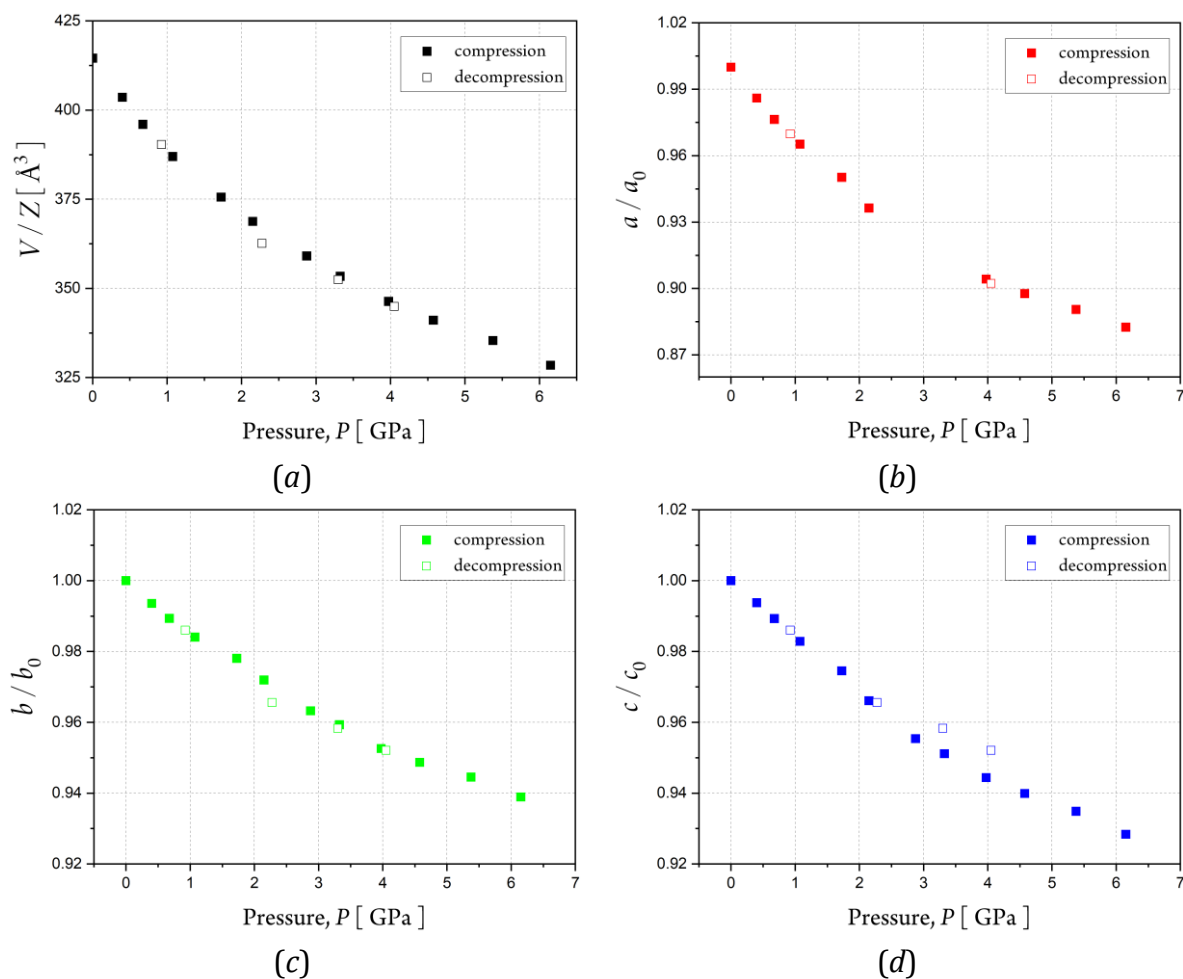


**Figure S6.1.**  $V/Z$  (a) and relative unit-cell changes ( $b,c,d$ ) vs. pressure. Both compression and decompression points are shown. For  $V/Z$  the best description of the curve is obtained with the 2<sup>nd</sup>-order polynomial fit. For unit-cell changes  $a_0$ ,  $b_0$  and  $c_0$  denote values from the ambient pressure measurement in DAC (**Ni-diONO-01-I**). For the  $a$  parameter points for phase **II** are not shown – these unit-cell parameter changes are large and  $a/a_0$  exceeds 1.4. In all cases estimated error bars are comparable to the symbols used, thus are not shown.

**Comment.** Calculation of crystal voids for disordered structures is not straightforward. Here this was accomplished with the *CRYSTALEXPLORER* software (settings: high-quality surface,  $0.002 \text{ e} \cdot \text{\AA}^{-3}$  electron-density cut-off). In the case of phases **I** and **II** one part of the disordered fragment was removed from the structure, and the voids were computed as for a standard ordered structure. The calculation of this kind was repeated for the other conformation of the disordered moiety. The overall void volume of the disordered structure was then calculated as a weighted average of the previously computed voids (weights were equal to the disorder occupancies).



**Table S6.1.** Crystal voids' volumes within the crystal structure during compression of the sample and its relationship to the overall unit-cell volume.

| Pressure, $P$ [ GPa ] | Phase      | $V_{\text{void}}$ [ $\text{\AA}^3$ ] | $V_{\text{void}}/V$ |
|-----------------------|------------|--------------------------------------|---------------------|
| ambient               | <b>I</b>   | 83.42                                | 0.050               |
| 0.40(5)               | <b>I</b>   | 61.43                                | 0.038               |
| 0.68(3)               | <b>I</b>   | 59.78                                | 0.038               |
| 1.08(3)               | <b>I</b>   | 47.36                                | 0.031               |
| 1.73(3)               | <b>I</b>   | 33.08                                | 0.022               |
| 2.15(5)               | <b>I</b>   | 25.80                                | 0.017               |
| 2.88(2)               | <b>II</b>  | 32.13                                | 0.015               |
| 3.33(3)               | <b>II</b>  | 25.73                                | 0.012               |
| 3.98(2)               | <b>III</b> | 12.18                                | 0.009               |
| 4.58(2)               | <b>III</b> | 9.58                                 | 0.007               |
| 5.38(3)               | <b>III</b> | 6.95                                 | 0.005               |
| 6.15(5)               | <b>III</b> | 4.28                                 | 0.003               |

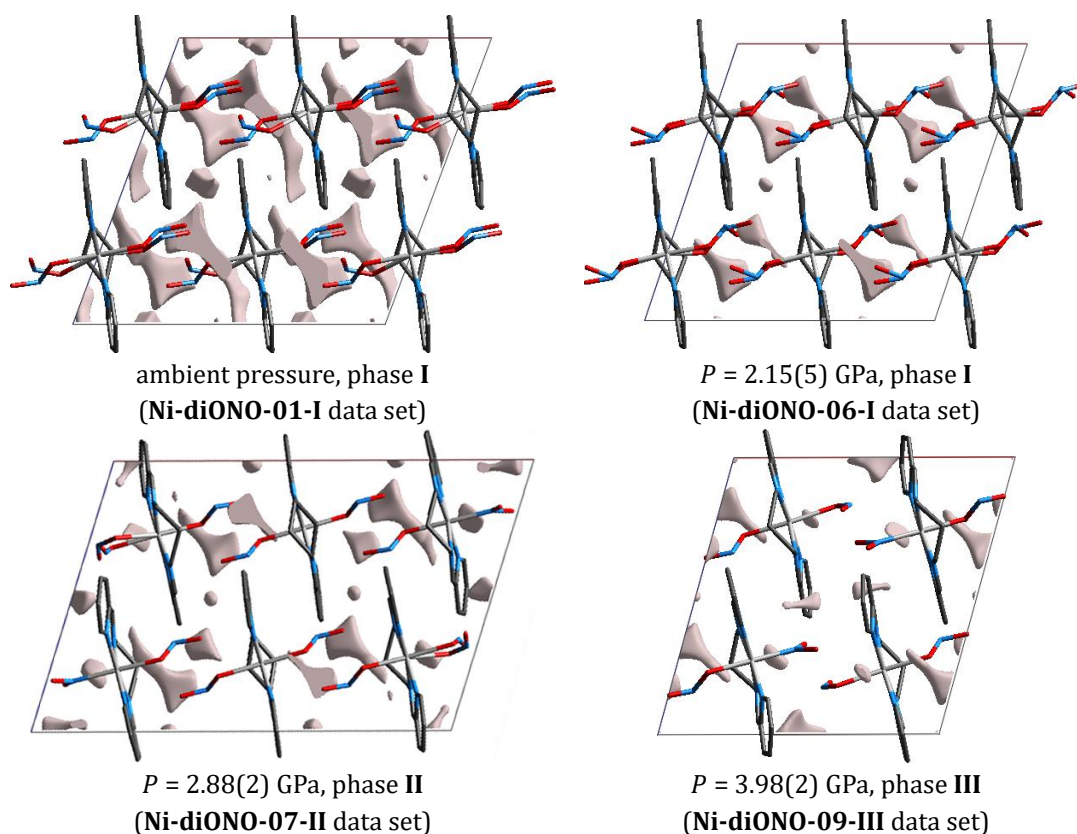


**Figure S6.2.** Crystal voids within the crystal structure at different pressure points, calculated per single unit cell (see Table S6.1).

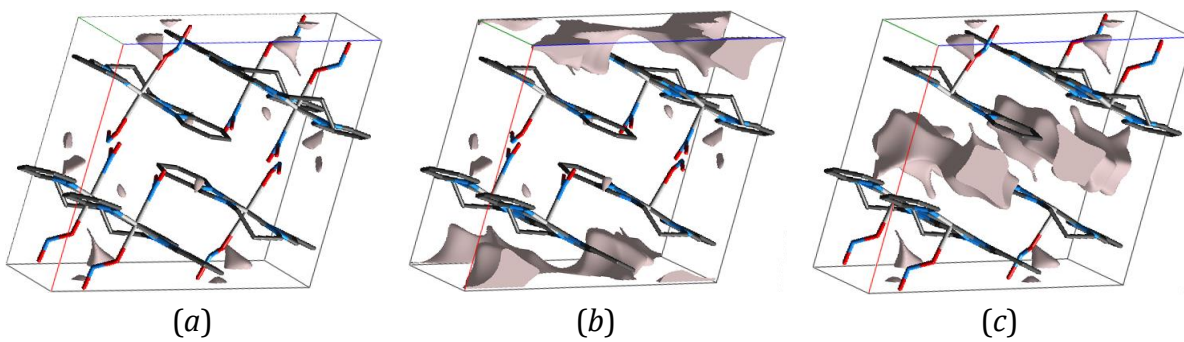


**Figure S6.3.** Crystal voids for the crystal structure at 6.15(5) GPa: (a) without cut-out NO<sub>2</sub> groups: 4.28 Å<sup>3</sup>; (b) with the *exo*-nitrito groups cut-out: 65.71 Å<sup>3</sup>; (c) with the *endo*-nitrito and nitro groups cut-out: 70.15 Å<sup>3</sup>.

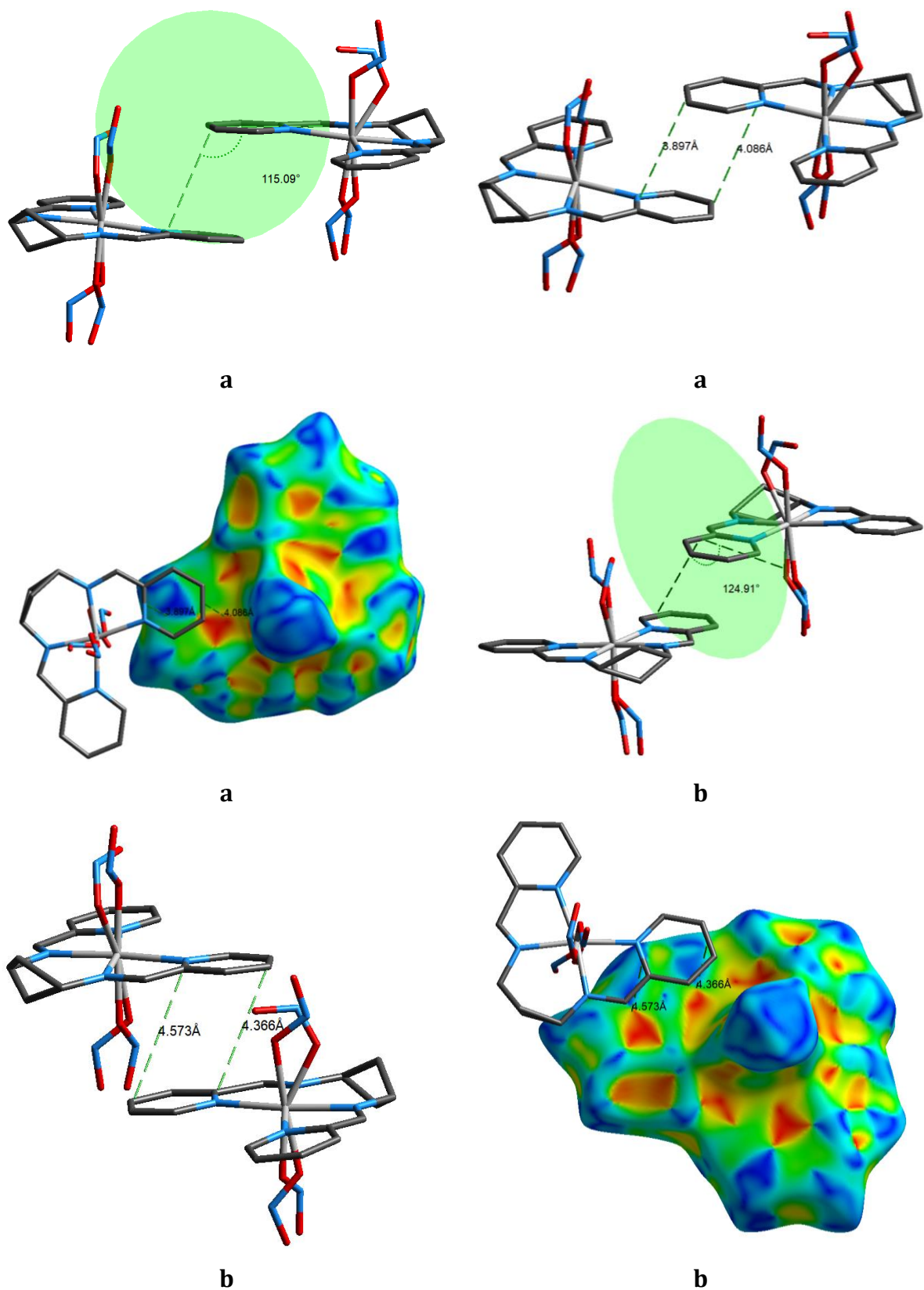


**Figure S6.4.** The  $\pi \cdots \pi$  stacking interactions observed in the structure of Ni-diONO at ambient pressure at r.t. (phase I). Some panels are redundant and show the same pattern with different descriptors, or in a different orientation.

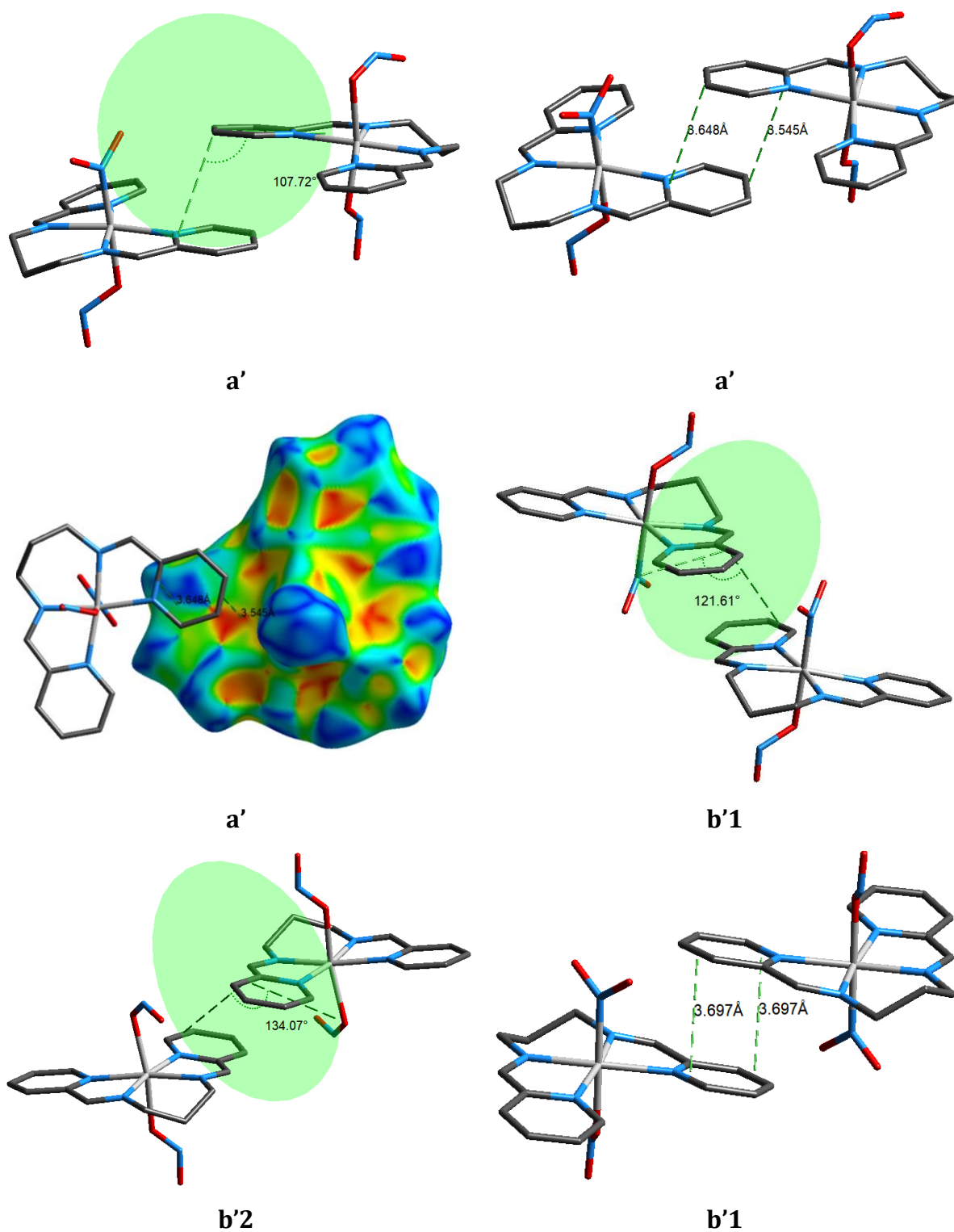


**Figure S6.5.** The  $\pi \cdots \pi$  stacking interactions observed in the structure of Ni-diONO at 3.98(2) GPa at r.t. (phase III). Some panels are redundant and show the same pattern with different descriptors, or in a different orientation.

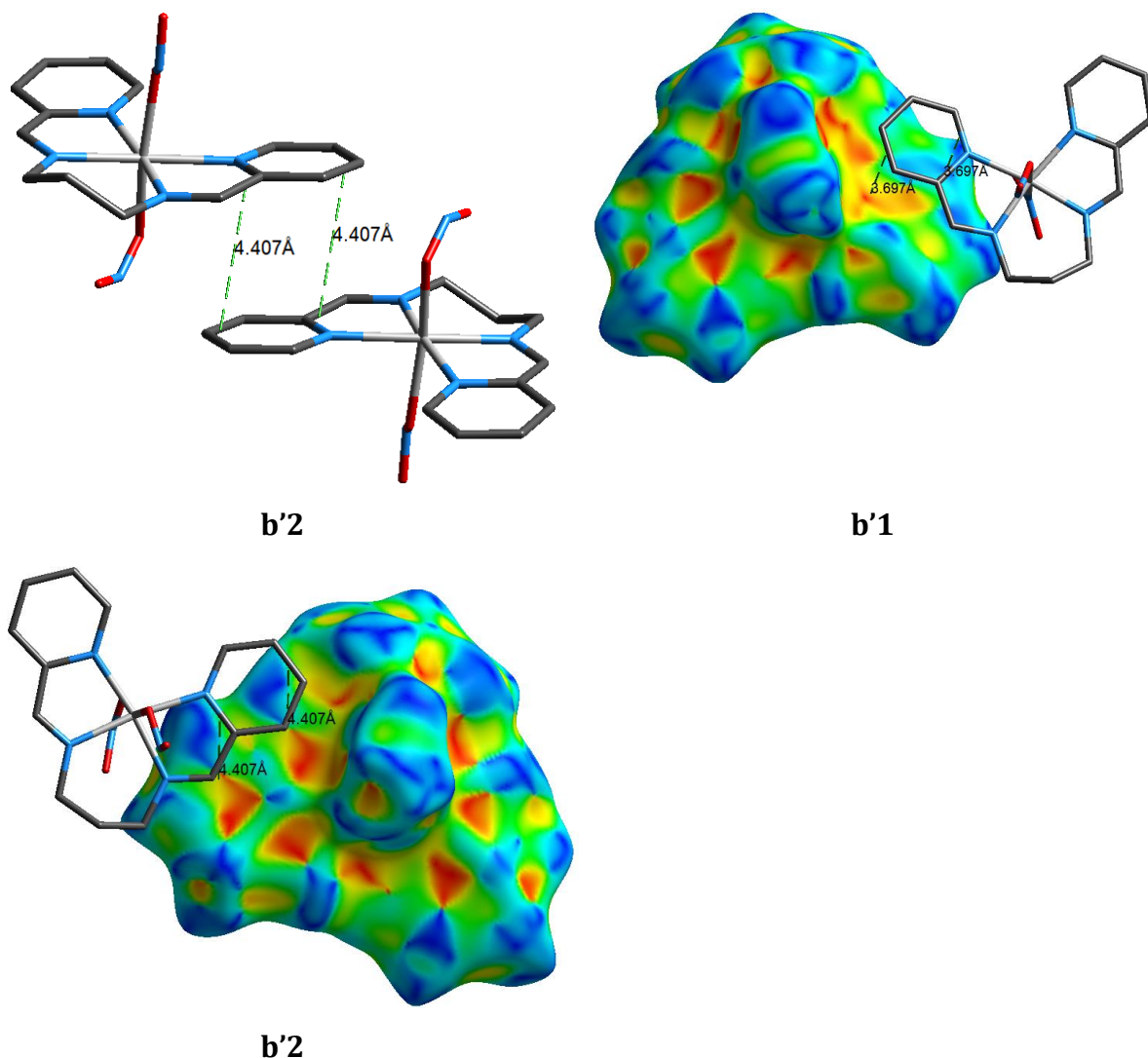


**Figure S6.5 (continued).** The  $\pi\cdots\pi$  stacking interactions observed in the structure of **Ni-diONO** at 3.98(2) GPa at r.t. (phase **III**). Some panels are redundant and show the same pattern with different descriptors, or in a different orientation.

**Comment.** Two types of  $\pi\cdots\pi$  interactions can be distinguished for the crystal structure of **Ni-diONO** at ambient pressure. Type **a** is more face-to-face stacked, and type **b** is more parallel displaced kind of  $\pi\cdots\pi$  interaction. As the pressure is applied the molecular fragments forming type **a'** interactions are pushed closer and the  $\pi$ -stacking character becomes more evident. This is also reflected on the Hirshfeld surface as the blue and red triangles become a bit more intense. However, in the case of **b**-type  $\pi\cdots\pi$  interactions the effect of pressure is more complex. The pressure-induced linkage isomerism leads to the molecule differentiation into two isomers. The molecules

exhibiting the nitro binding mode which are involved in the type **b'1**  $\pi \cdots \pi$  interaction slide closer one to another, thus the distances between aromatic rings get significantly more reduced than in the case of molecules with the *endo*-nitrito binding mode (**b'2**), which slide away from each other. The pressure impact is well visible on the respective Hirshfeld surfaces. In the case of **b'1** red and blue triangles become more faded and for **b'2** more intense in comparison to **b**.

## 7. Principal-axis strain-tensor analysis

**Comment.** The analyses presented below were performed with the PASCAL Python-written web-based tool (Cliffe & Goodwin, 2012, Lertkiattrakul *et al.*, 2023). Given the reasonable number of available pressure points, the analysis was conducted only for the phase **I**. Since this phase belongs to the monoclinic space group, it could be informative to provide not only the changes of the unit-cell parameters, but also the strain-tensor principal-axes lengths' changes (Figure S7.1). Note the obtained relative changes agree well with the unit-cell changes quoted in the main text (taking into account the obliquity of the crystal system).

The program also fits the Birch-Murnaghan equation of fit of both 2<sup>nd</sup> and 3<sup>rd</sup> order. The results are presented in Table 7.1. The obtained bulk modulus is typical for metal complexes.

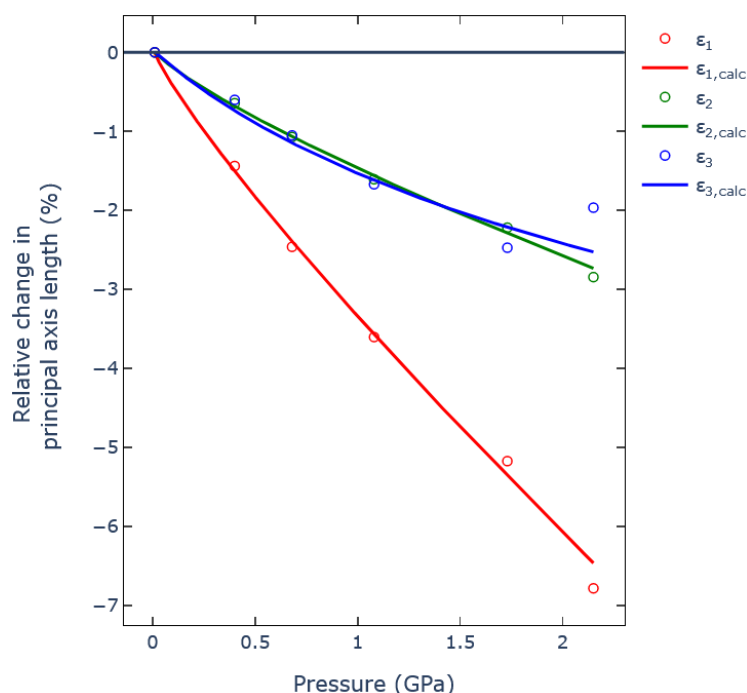


**Figure 7.1.** Relative changes in the principal axis length for the phase **I** vs. pressure.



**Table 7.1.** The calculated Birch-Murnaghan equation-of-state coefficients for the phase I.

| Order           | $B_0$ [GPa] | $\sigma(B_0)$ [GPa] | $V_0$ [ $\text{\AA}^3$ ] | $\sigma(V_0)$ [ $\text{\AA}^3$ ] | $B'$  | $\sigma(B')$ |
|-----------------|-------------|---------------------|--------------------------|----------------------------------|-------|--------------|
| 2 <sup>nd</sup> | 14.132      | 0.2497              | 1658.8                   | 1.3208                           | 4     | n/a          |
| 3 <sup>rd</sup> | 12.476      | 0.3273              | 1659.6                   | 0.5587                           | 6.608 | 0.553        |

## 8. Theoretical UV-Vis spectra

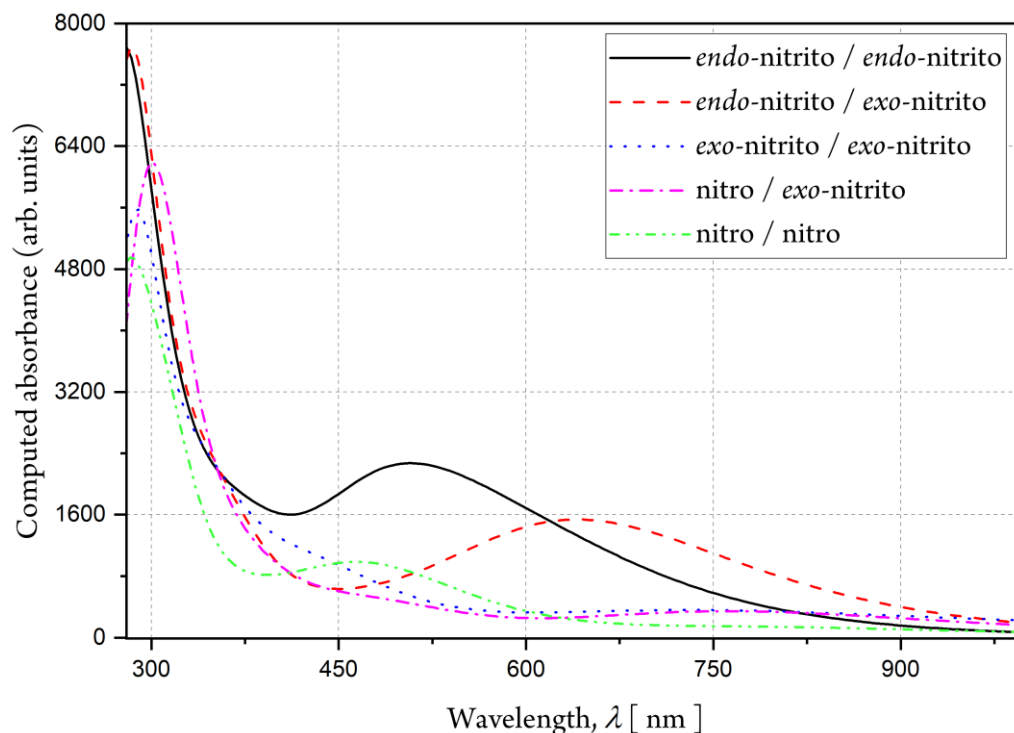


**Figure S8.1.** Theoretical UV-Vis spectra calculated for selected possible isomeric forms (DFT(B3LYP)/6-311++G\*\* level of theory, optimised geometries). Note that for the nitro and *endo*-nitrito forms low-energy bands are red-shifted compared to the *exo*-nitrito form. Therefore isomerisation may to some extent contribute to the pressure-induced crystal colour change. For isomers' description see comment below Table S4.1.

## 9. Additional references

- Allen, F. H. (2002). *Acta Cryst. Sect. B* **58**, 380-388.
- Becke, A. D. (1988). *Phys. Rev. A* **38**, 3098-3100.
- Boys, S. F. & Bernardi, F. (1970). *Mol. Phys.* **19**, 553-566.
- Campbell, T. G. & Urbach, F. L. (1973). *Inorg. Chem.* **12**, 1836-1840.
- Clark, T., Chandrasekhar, J., Spitznagel, G. W. & Schleyer, P. v. R. (1983). *J. Comput. Chem.* **4**, 294-301.
- Cliffe, M. J. & Goodwin, A. L. (2012). *J. Appl. Cryst.* **45**, 1321-1329.
- Dolomanov, O. V., Bourhis, L. J., Gildea, R. J., Howard, J. A. K. & Puschmann, H. (2009). *J. Appl. Cryst.* **42**, 339-341.
- Frisch, M. J., Trucks, G. W., Schlegel, H. B., Scuseria, G. E., Robb, M. A., Cheeseman, J. R., Scalmani, G., Barone, V., Petersson, G. A., Nakatsuji, H., Li, X., Caricato, M., Marenich, A. V., Bloino, J., Janesko, B. G., Gomperts, R., Mennucci, B., Hratchian, H. P., Ortiz, J. V., Izmaylov, A. F., Sonnenberg, J. L., Williams, Ding, F., Lipparini, F., Egidi, F., Goings, J., Peng, B., Petrone, A., Henderson, T., Ranasinghe, D., Zakrzewski, V. G., Gao, J., Rega, N., Zheng, G., Liang, W., Hada, M., Ehara, M., Toyota, K., Fukuda, R., Hasegawa, J., Ishida, M., Nakajima, T., Honda, Y., Kitao, O., Nakai, H., Vreven, T., Throssell, K., Montgomery Jr, J. A., Peralta, J. E., Ogliaro, F., Bearpark, M. J., Heyd, J. J., Brothers, E. N., Kudin, K. N., Staroverov, V. N., Keith, T. A., Kobayashi, R., Normand, J., Raghavachari, K., Rendell, A. P., Burant, J. C., Iyengar, S. S., Tomasi, J., Cossi, M., Millam, J. M., Klene, M., Adamo, C., Cammi, R., Ochterski, J. W., Martin, R. L., Morokuma, K., Farkas, O., Foresman, J. B. & Fox, D. J. (2016). *GAUSSIAN 16*.
- Grimme, S. (2004). *J. Comput. Chem.* **25**, 1463-1473.
- Grimme, S. (2006). *J. Comput. Chem.* **27**, 1787-1799.
- Grimme, S., Antony, J., Ehrlich, S. & Krieg, H. (2010). *J. Chem. Phys.* **132**, 154104.
- Grimme, S., Ehrlich, S. & Goerigk, L. (2011). *J. Comput. Chem.* **32**, 1456-1465.
- Groom, C. R., Bruno, I. J., Lightfoot, M. P. & Ward, S. C. (2016). *Acta Cryst. Sect. B* **72**, 171-179.
- Kamiński, R., Jarzemska, K. N. & Domagała, S. (2013). *J. Appl. Cryst.* **46**, 540-534.
- Lee, C., Yang, W. & Parr, R. G. (1988). *Phys. Rev. B* **37**, 785-789.
- Lertkiattrakul, M., Evans, M. L. & Cliffe, M. J. (2023). *J. Open Source Softw.* **8**, 5556.
- McLean, A. D. & Chandler, G. S. (1980). *J. Chem. Phys.* **72**, 5639-5648.
- Perdew, J. P. (1986). *Phys. Rev. B* **33**, 8822-8824.
- Petříček, V., Dušek, M. & Palatinus, L. (2014). *Z. Kristallogr.* **229**, 345-352.
- Rigaku Oxford Diffraction (2024). *CRYSTALIS PRO*.
- Sheldrick, G. M. (2008). *Acta Cryst. Sect. A* **64**, 112-122.
- Sheldrick, G. M. (2015). *Acta Cryst. Sect. A* **71**, 3-8.
- Spackman, M. A. & Jayatilaka, D. (2009). *CrystEngComm* **11**, 19-32.